WKB Analysis of Tunnel Coupling in a Simple Model of a Double Quantum Dot

by

Edward L. Platt

A thesis
presented to the University of Waterloo
in fulfillment of the
thesis requirement for the degree of
Master of Mathematics
in
Applied Mathematics

Waterloo, Ontario, Canada, 2008

I hereby declare that I am the sole author of this thesis. This is a true copy of the thesis, including any required final revisions, as accepted by my examiners.

I understand that my thesis may be made electronically available to the public.

Abstract

A simplified model of a double quantum dot is presented and analyzed, with applications to spin-qubit quantum computation. The ability to trap single electrons in semiconductor nanostructures has led to the proposal of quantum computers with spin-based qubits coupled by the exchange interaction. Current theory predicts an exchange interaction with a ϵ^{-1} dependence on the detuning ϵ, the energy offset between the two dots. However, experiment has shown an $\epsilon^{-3/2}$ dependence. Using WKB analysis, this thesis explores one possible source of the modified dependence, namely an ϵ-dependent tunnel coupling between the two wells. WKB quantization is used to find expressions for the tunnel coupling of a one-dimensional double-well, and these results are compared to the exact, numerical solutions, as determined by the finite difference method and the transfer matrix method. Small ϵ-dependent corrections to the tunnel coupling are observed. In typical cases, WKB correctly predicts a constant tunnel coupling at leading-order. WKB also predicts small ϵ-dependent corrections for typical cases and strongly ϵ-dependent tunnel couplings for certain exceptional cases. However, numerical simulations suggest that WKB is not accurate enough to analyze the small corrections, and is not valid in the exceptional cases. Deviations from the conventional form of the low-energy Hamiltonian for a double-well are also observed and discussed.

Acknowledgements

I would like to thank my advisors, Josef Paldus and Frank Wilhelm, for continuing guidance and feedback over the course of my research. I also thank William A. Coish for his role as my unofficial advisor and all of the assistance and knowledge he has provided. Thanks to Helen Warren of the Applied Math Graduate Office for indispensable help and answers to many questions. Thanks also, to Edward R. Vrscay and Marcel Nooijen for feedback and suggestions. I would also like to acknowledge the free and open source software community for creating much of the software I use, including LaTeX, PyXPlot, and Inkscape. Finally, I would like to thank Sharon Ouellette for her support, patience, and inspiration, as well as my parents for all of their support.

Contents

List of Tables

List of Figures

Chapter 1

Introduction

Double-well potentials have long been a subject of study in quantum mechanics. Recently however, advances in nanotechnolgy and quantum computation have motivated new questions about the behavior of particles in these potentials. In particular, it is now possible to trap single electrons in nanostructures called *quantum dots*. The ability to trap and manipulate single electrons has important applications in the development of a quantum computer, a device theorized to solve certain problems significantly faster than classical computers.

Such a device requires quantum two-state systems, called *qubits*, to store information, as well as a systematic method for controlling the interactions between these qubits. A double quantum dot, in which two electrons are trapped in adjacent potential wells, is one of the simplest systems exhibiting both properties. Each electron's spin represents a two-state system which can be used as a qubit, while the exchange interaction between the two electrons can be controlled by changing the confinement potential. It is thus desirable to understand precisely how the parameters of the confinement potential influence the strength of the exchange interaction.

In the limit of negligible Coulomb interaction, the strength of the exchange interaction can be quantified in terms of two parameters of the potential: the detuning and the tunnel

coupling. The *detuning* is the offset between the energy levels of the two potential wells, and can be varied experimentally by placing electrodes at each well and applying a voltage. The *tunnel coupling* measures the delocalization of the energy eigenstates due to tunneling across the potential barrier. The tunnel coupling is usually assumed to be constant, but experimental results have brought this assumption into question. The primary focus of this thesis is to determine, using Wentzel-Kramers-Brillouin (WKB) analysis, whether there is any detuning-dependence of the tunnel coupling.

1.1 Quantum computation with quantum dots

A quantum dot, sometimes called an "artificial atom," is any device capable of trapping a single electron (or small number of electrons) in a localized potential well [2]. There are many different ways of constructing such devices. A *lateral quantum dot* (Figure 1.1), the type most relevant to this thesis, consists of two semiconductor layers with metal electrodes placed on top. The boundary between the two types of semiconductor, a *heterojunction*, confines the electrons to a plane, creating a two-dimensional electron gas (2DEG). The electrodes then create a tunable confinement potential within that plane. Other types of quantum dots include *vertical quantum dots*, for which the confinement potential is created entirely by heterojunctions. The confinement of single electrons in both lateral and vertical quantum dots has been realized experimentally [6, 25]. Other types include self-assembled quantum dots [10] and nanotube quantum dots [4, 24].

If a quantum dot is an artificial atom, then two next to each other can be considered an artificial molecule. Such a configuration is called a double quantum dot. Depending on the height of the barrier separating the two dots, their energy eigenstates may hybridize to create delocalized "molecular orbitals." Double quantum dots [9, 15, 21], and even triple quantum dots [11, 22] have been experimentally realized.

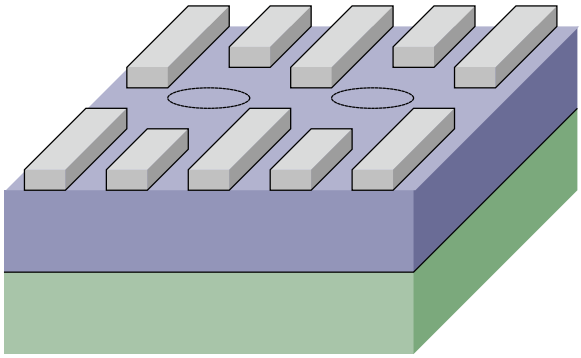

Figure 1.1: Schematic illustration of a lateral double quantum dot. Electrons are confined to the 2-dimensional plane created by a heterojunction of two types of semiconductor. Electrodes are then used to create a confinement potential within this plane, and trap individual electrons.

Quantum computation is a model of computation based on the rules of quantum mechanics, rather than those of Boolean logic (the foundation of classical computation). Quantum information is thus stored in *qubits*, which, unlike classical bits, can exist in superpositions and entangled states. The observation that it is computationally hard for classical computers to simulate quantum systems led to the conjecture that the rules of quantum mechanics are computationally more powerful than the rules of classical logic. In fact, several quantum algorithms have been discovered that offer computational speedup over any known classical algorithms [19], including the Deutsch-Jozsa algorithm, the Grover search algorithm, and Shor's prime factorization algorithm. Shor's algorithm has stimulated interest in quantum computation because an efficient method for prime factorization could be used to break RSA encryption, one of the most popular public-key encryption schemes.

However, several obstacles stand in the way of large-scale quantum computation. To design a quantum computer, one must choose a physical system to use as a qubit. It must be possible to reliably control and measure the states of these qubits. Furthermore, techniques

must exist to prevent decoherence, the tendency of quantum states to transition into classical ones. As a practical matter, it must also be possible to reliably fabricate a large number of qubits with the necessary interconnections. No system is ideal, but quantum dots are one potential candidate for a practical qubit.

Two types of quantum-dot qubits have been proposed: spin qubits and charge qubits. In a spin qubit, the qubit is encoded in the spin of an electron in a quantum dot [7]. Two such qubits can be coupled via the exchange interaction, allowing the implementation of two-qubit computational operations [5]. Alternatively, in a charge qubit, information is encoded by which side of a double quantum dot an electron is in [15].

1.2 Exchange interaction and tunnel coupling

Coupling between lateral quantum dot spin qubits is achieved using the exchange interaction. The exchange interaction is a purely quantum mechanical "pseudo-force" acting on identical fermions. As identical fermions, the wave function of any two electrons must be antisymmetric under exchange. The Pauli exclusion principle arises as a result: two electrons with parallel spin states cannot exist in the same orbital state. Thus, if there are only two orbital states under consideration, with one electron in each orbital, the Hamiltonian may be written as:

$$H = J\vec{S}^{(1)} \cdot \vec{S}^{(2)}, \tag{1.1}$$

where J is the difference between the energies of the spin singlet and spin triplet states, and $S^{(i)}$ is the spin operator acting on electron i. This interaction, arising from the quantum mechanical properties of fermions under exchange, is called the exchange interaction.

The exchange interaction for two electrons in a double quantum dot can be related to

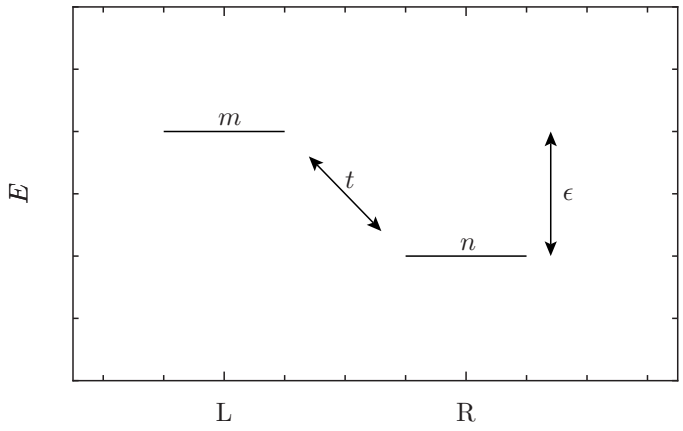

Figure 1.2: Schematic diagram of the Hubbard model of a double quantum dot. The ground-state energy levels of the left and right dots are separated by an energy detuning ϵ. The occupation numbers of the left and right dots are m and n respectively. The strenght of tunneling between the two quantum dots is quantified by the tunnel coupling, t.

the tunnel coupling of the dot. The calculation can be done by modelling the system by a Hubbard Hamiltonian (Figure 1.2). Let (m, n) be the state of a double quantum dot, where m is the ground-state occupation number of higher-energy well, and n is the ground-state occupation number of the lower well. In a low-energy, detuned quantum dot, we can assume that the $(1, 1)$ and $(0, 2)$ states are the only energetically allowed configurations. A spin singlet (antisymmetric state) can exist in both states, however a spin triplet (symmetric state) cannot exist in the $(0, 2)$ state due to the exclusion principle. Tunneling between the $(1, 1)$ and $(0, 2)$ states thus perturbatively lowers the energy for the $(1, 1)$ spin singlet, while leaving the energy of the $(1, 1)$ spin triplet unchanged. The difference in singlet and triplet energies is exactly the strength of the exchange interaction J, and is given by:

$$J = \frac{t^2}{2\epsilon}, \tag{1.2}$$

where t is the tunnel coupling, and the detuning ϵ is the energy offset difference between the $(1, 1)$ and $(0, 2)$ configurations. Note that some authors use "tunnel coupling" to refer

to $t' = 2t$. In the limit of weak Coulomb interaction, both t and ϵ can be determined from the case of a single electron in a double-well potential. We thus focus on the single-electron case for the majority of this thesis, bearing in mind this connection to the two-electron case.

The tunnel coupling is usually assumed to be independent of detuning, resulting in an exchange interaction proportional to ϵ^{-1}. However, the observation of an exchange interaction proportional to $\epsilon^{-3/2}$ [16] suggests the possibility of an ϵ-dependent tunnel coupling. This thesis is thus devoted to exploring ways in which an ϵ-dependent tunnel coupling could arise.

1.3 Modelling quantum dots

We use a significantly simplified model for a quantum dot: a one-dimensional, double-well potential. One simplification we make is the effective mass approximation [14]. Semiconductors are crystals, with each atom in the crystal presenting a local potential minimum to electrons, so even a single quantum dot contains many potential wells. The effective mass approximation replaces the periodic crystalline potential with a constant potential, and replaces the mass of the electron with an effective mass that depends on the particular semiconductor material. This approximation is used extensively in solid-state physics, and allows us to ignore the crystal structure of the semiconductor and focus on the shape of the confinement potential.

The confinement potential is clearly three-dimensional, but may be approximated by a one-dimensional potential for low-energy electrons and sufficiently strong confinement in the other two dimensions. A lateral double quantum dot can be approximated as having three independent Hamiltonian components: one for the semiconductor heterojunction (z direction), one single well (y direction), and one double well (x direction). The energy spectrum of the double well consists of doublets, separated by a characteristic energy spacing.

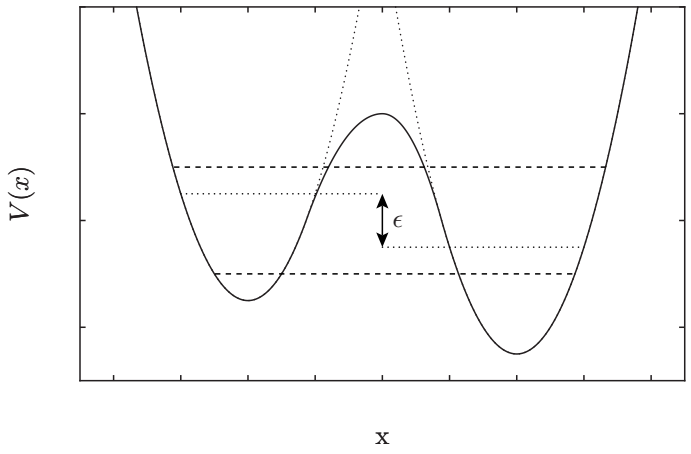

Figure 1.3: Schematic plot of the double-well potential used to represent a double quantum dot. The dotted lines show the energies of single-wells centered around the left and right halves of the double-well. The offset between these energy levels is the detuning ϵ. The dashed lines show the energy levels of the double-well.

The single well, and heterojunction spectra each consist of single states separated by a characteristic energy spacing, equal to or larger than that of the double well. Thus, if the energy of the system is less than these characteristic energies, the lowest doublet of the double well provides the only degree of freedom and the other Hamiltonian components may be ignored. This leaves us with our simplified, one-dimensional double well model (Figure 1.3). We use the convention that the detuning ϵ is positive when the left well is higher. Note that due to tunneling, the energy levels are pushed apart relative to where the levels of similarly shaped single-wells would be. By applying WKB analysis to this model, we find and test expressions for the tunnel coupling to see if they show any ϵ-dependence.

1.4 Overview of chapters

In Chapter 2 we begin by discussing tunneling in a one-dimensional double-well and formally defining the tunnel coupling. We then review WKB energy quantization in Chapter 3 and use it to derive expressions for tunnel coupling in Chapter 4. We review numerical methods

in Chapter 5 and discuss numerical simulations used to test the detuning-dependence of the tunnel coupling in Chapter 6 and Chapter 7. Finally, we conclude and discuss future directions in Chapter 8.

Chapter 2

Tunneling in a 1-D Double-Well

In this chapter, we discuss the behavior of a particle bound in a double-well potential. A typical bound state in a double-well has two *classically allowed regions*, where the potential energy is less than the particle energy. These regions are separated by a *classically forbidden region*, or barrier, where the potential energy is larger than the particle energy. Quantum mechanics predicts that a particle travelling in such a potential is most likely to be found in the allowed regions. However, unlike classical mechanics, quantum mechanics predicts that a particle can also be found in the forbidden region. This uniquely quantum mechanical behavior allows a particle, initially localized in one potential well, to penetrate through the barrier, into the other well. This process is known as *quantum tunneling*. We discuss the effects of tunneling on the solutions of a double-well, and quantify the strength of tunneling effects by defining the "tunnel coupling." We focus on the parameters regime in which the double-well can be approximated as a two-state system for particles of sufficiently low energy.

First, we formally discuss the potential of the double-well (Section 2.1). We then introduce several sets of basis states (Section 2.2) and use them to construct the state-space representation of the full, double-well Hamiltonian (Section 2.3). Subsequently, we construct a reduced Hamiltonian for a low-energy particle in a double-well (Section 2.4) and discuss

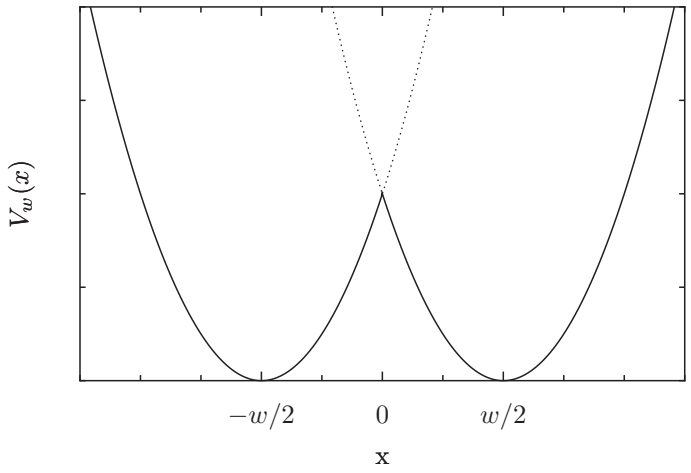

Figure 2.1: An example of a double-well potential constructed from two single-well potentials centered at $\pm w/2$. In this diagram, a parabolic potential has been chosen for both single-well potentials $V_L(x)$ and $V_R(x)$. In general however, the two wells need not have the same shape.

the implications of its energy spectrum (Section 2.5).

2.1 The double-well potential

We begin by defining the double-well potential in terms of two single-well potentials. Let $V_L(x)$ and $V_R(x)$ be two single-wells, each with a minimum at $x = 0$. Also let H_L and H_R be the Hamiltonians corresponding to $V_L(x)$ and $V_R(x)$ respectively. We define a family of double-well potentials $V_w(x)$ such that:

$$V_w(x) \quad = \quad \begin{cases} V_L(x + w/2) & x < 0, \\ V_R(x - w/2) & x > 0. \end{cases} \tag{2.1}$$

The resulting potential (Figure 2.1) is a double-well with minima separated by a width w. Note that $V_w(x)$ could be discontinuous or have discontinuous derivatives at $x = 0$. However, a smoothing function could be added to $V_w(x)$ without changing the following analysis.

The parameter w controls the size of the barrier, and thus the strength of the tunneling. In the limit $w \to \infty$, the barrier becomes infinite and no tunneling can occur. In this case, the system becomes equivalent to two single-wells, $V_L(x)$ and $V_R(x)$, in isolation. Thus, as w increases, the eigenstates and energy levels for the double-well must approach those of the single-wells. In other words, for the case of a large barrier, the potential can be treated as two single-wells coupled by the effects of tunneling. When this coupling is weak, we can treat it as a perturbation and significantly simplify the Hamiltonian.

2.2 Double-well basis states

We wish to transform the continuous position-space Hamiltonian of the double-well into an equivalent, discrete, state-space Hamiltonian. To accomplish this, we must first choose a set of basis states in which to write this new Hamiltonian. Since we plan to treat tunneling as a perturbation of two isolated single-wells, we desire basis states that approach the unperturbed eigenstates of H_L and H_R as the size of the barrier is increased.

We begin with the eigenstates of H_L and H_R themselves, which we will refer to as the *single-well states*. We denote these states as $|\phi_{L,m}\rangle$ and $|\phi_{R,n}\rangle$ with energy levels $E_{L,m}$ and $E_{R,n}$ respectively. Although these states have the correct infinite-barrier behavior, they do not form an orthonormal basis for a finite barrier. Each of $\{|\phi_{L,m}\rangle\}$ and $\{|\phi_{R,n}\rangle\}$ are complete orthonormal sets by themselves, therefore their union is overcomplete, and necessarily non-orthogonal. However, for a large barrier, $\langle\phi_{L,m}|\phi_{R,n}\rangle$ will be small for all m, n. Therefore, if we use a procedure such as Graham-Schmidt orthonormalization, the corrections to the single-well states will be small, and tend to zero as the barrier is increased, as required. Each resulting basis state will also be highly localized around either the left or right well, so we will refer to this set of states as the *localized basis*. We denote the localized basis states as

$|\psi_{L,m}\rangle$ and $|\psi_{R,n}\rangle$, such that:

$$|\psi_{L,m}\rangle \to |\phi_{L,m}\rangle \qquad \text{as } w \to \infty, \tag{2.2}$$

$$|\psi_{R,n}\rangle \to |\phi_{R,n}\rangle \qquad \text{as } w \to \infty. \tag{2.3}$$

A third set of states is necessary for our analysis of the double-well Hamiltonian, namely the full energy eigenstates of the double-well. We refer to these states as the *double-well states* and denote them as $|\psi_{I,n}\rangle$ and $|\psi_{II,m}\rangle$ with the corresponding energy levels $E_{I,n}$ and $E_{II,m}$. Note that in the limit of an infinite barrier, these states must also approach the single-well states:

$$|\psi_{I,n}\rangle \to |\phi_{R,n}\rangle \qquad \text{as } w \to \infty, \tag{2.4}$$

$$|\psi_{II,m}\rangle \to |\phi_{L,m}\rangle \qquad \text{as } w \to \infty, \tag{2.5}$$

where equating $|\psi_{I,n}\rangle$ with $|\psi_{R,n}\rangle$ corresponds to the convention that, for positive detuning, the ground state of the left single-well is higher than that of the right

Each set of states, the single-well states, the localized basis, and the double-well basis, plays an important role in our construction and analysis of the double-well Hamiltonian.

2.3 Double-well Hamiltonian

We seek to write the double-well Hamiltonian as

$$H \;=\; H^{(S)} + H^{(T)}, \tag{2.6}$$

where $H^{(S)}$ is the Hamiltonian of two isolated single-wells, and $H^{(T)}$ is a small perturbation describing the effects of tunneling. The localized basis derived in Section 2.2 allows us to

write the Hamiltonian in such a form. The elements of the Hamiltonian in this basis can be written in terms of the position-space wavefunctions of the states:

$$\begin{aligned} H_{A,m;B,n} &= \langle \psi_{A,m} | H | \psi_{B,n} \rangle, & (2.7) \\ &= \int_{-\infty}^{\infty} dx\, \psi_{A,m}(x) H_x \psi_{B,n}(x), & (2.8) \end{aligned}$$

where $A, B \in \{L, R\}$, and H_x is the position-space Hamiltonian.

We consider the diagonal and off-diagonal matrix elements separately. For weak tunneling, the basis states are very close to the single-well eigenstates, and the diagonal matrix elements will be very close to the energy eigenvalues of the single-wells:

$$\begin{aligned} \langle \psi_{A,m} | H | \psi_{A,m} \rangle &\approx \langle \phi_{A,m} | H_A | \phi_{A,m} \rangle & (2.9) \\ &= E_{A,m}. & (2.10) \end{aligned}$$

We may thus write the diagonal elements as the single-well energies plus some small perturbation:

$$\begin{aligned} H_{A,m,A,m} &= H^{(S)}_{A,m,A,m} + H^{(T)}_{A,m,A,m}, & (2.11) \\ H^{(S)}_{A,m,A,m} &= E_{A,m}, & (2.12) \\ H^{(T)}_{A,m,A,m} &\equiv \langle \phi_{A,m} | H_A | \phi_{A,m} \rangle - E_{A,m}, & (2.13) \end{aligned}$$

which has the desired form (2.6).

In the weak tunneling regime, all off-diagonal elements will be small, and can be included in the $H^{(T)}$ portion of the Hamiltonian. Off-diagonal elements that couple two states localized in the same well will be small because the states are very close to orthogonal single-well eigenstates. Off-diagonal elements that couple two states localized in different wells are

suppressed by the barrier, and thus become small as tunneling becomes weak.

This completes the construction of the double-well Hamiltonian as a single-well Hamiltonian $H^{(S)}$ plus a tunneling perturbation $H^{(T)}$. Note that although the state-space representation of $H^{(S)}$ is equal to that of a Hamiltonian for two isolated single-wells, they are not written in the same basis. For two isolated single-wells, the Hamiltonian corresponds to the single-well basis, while the double-well $H^{(S)}$ is written in the localized basis. $H^{(S)}$ then does not physically correspond to two widely separated single-wells. However, $H^{(S)}$ has the same spectrum as the Hamiltonian for two isolated single-wells, so we may still use it for our analysis.

2.4 Reduced Hamiltonian

Having written the full double-well Hamiltonian as a single-well portion plus a perturbation due to tunneling, we could use standard perturbation theory to describe the double-well energy levels $E_{I,n}$ and $E_{II,m}$ in terms of the single-well energies $E_{L,m}$ and $E_{R,n}$. However, we will focus on a special case that allows us to reduce the Hamiltonian to that of a two-state system, which can be solved exactly. As we focus on low-energy states, we will drop the numerical subscript from states and energies when it is "1" (e.g. $|\psi_L\rangle = |\psi_{L,1}\rangle$).

In particular, we focus on a regime in which the left and right well ground states are very close in energy, as well as very close to the total energy of the system. We define the *detuning* ϵ as the difference between the left and right single-well ground-state energy levels, and require that it be small compared to the single-well level spacing Δ:

$$|\epsilon| \ll \Delta, \tag{2.14}$$

$$\epsilon = E_L - E_R, \tag{2.15}$$

$$\Delta = \min\{(E_{L,2} - E_{L,1}), (E_{R,2} - E_{R,1})\}. \tag{2.16}$$

When the condition (2.14) is met, the ground states of the left and right wells are said to be *in resonance* or *resonant*. We limit our analysis to states $|\psi\rangle$, such that the expected energy of $|\psi\rangle$ is very close to the ground state of the double-well:

$$|\langle\psi|H|\psi\rangle - E_I| \;\ll\; \Delta \tag{2.17}$$

When the condition (2.17) is met, the system is very likely to be found in one of the lowest-energy double-well eigenstates $|\psi_I\rangle$ or $|\psi_{II}\rangle$. In other words, the system could be approximated by a reduced Hamiltonian acting on the subspace spanned by $|\psi_I\rangle$ and $|\psi_{II}\rangle$, and this approximation improves as the system is cooled to lower energies. Similarly, for the case of weak tunneling, the double-well basis and the localized basis approach each other, and the system is also very likely to be found in one of the localized states $|\psi_L\rangle$ or $|\psi_R\rangle$. We will construct our reduced Hamiltonian to act on the subspace spanned by these localized states. However, using the localized basis introduces additional approximation error, which becomes smaller as tunneling becomes weaker. We now construct the low-energy, reduced Hamiltonian for the localized basis and estimate its error.

The time-independent Schrödinger equation for a Hamiltonian H states that

$$H|\psi\rangle \;=\; E|\psi\rangle, \tag{2.18}$$

for each eigenstate $|\psi\rangle$ and its corresponding energy E. We seek a reduced Hamiltonian acting on the space spanned by the low-energy, localized states $|\psi_L\rangle$ and $|\psi_R\rangle$. We call this space $\mathcal{S}$ and define an idempotent projector P onto it,

$$P \;=\; |\psi_L\rangle\langle\psi_L| + |\psi_R\rangle\langle\psi_R|, \tag{2.19}$$

$$P^2 \;=\; P. \tag{2.20}$$

The ideal Schrödinger equation for the reduced Hamiltonian should have the form,

$$PHP|\psi\rangle = EP|\psi\rangle, \tag{2.21}$$

where H is the full double-well Hamiltonian, and PHP is the projection of the Hamiltonian onto the low-energy, localized subspace. However, we expect that there will be some tunneling-dependent error due to the reduction of the Hamiltonian, so we wish to write the Schrödinger equation as

$$PHP|\psi\rangle + H_E|\psi\rangle = EP|\psi\rangle, \tag{2.22}$$

where the error is represented by the operator H_E.

We begin by defining Q as the orthogonal complement of P and write two equations by multiplying (2.18) on the left by P and Q, respectively,

$$Q = I - P, \tag{2.23}$$

$$PH|\psi\rangle = EP|\psi\rangle, \tag{2.24}$$

$$QH|\psi\rangle = EQ|\psi\rangle. \tag{2.25}$$

We then insert $I = P + Q$ into each equation yielding

$$PHP|\psi\rangle + PHQ|\psi\rangle = EP|\psi\rangle, \tag{2.26}$$

$$QHP|\psi\rangle + QHQ|\psi\rangle = EQ|\psi\rangle. \tag{2.27}$$

Equation (2.26) is of the desired form (2.22). However, combining (2.26) and (2.27) allows us to derive another equation of the desired form, which results in a more informative error

estimate. Solving (2.27) for $Q|\psi\rangle$, noting that $Q^2 = Q$, gives:

$$\begin{aligned}
(EQ - QHQ)|\psi\rangle &= QHP|\psi\rangle, && (2.28)\\
(EQ - QHQQ)|\psi\rangle &= QHP|\psi\rangle, && (2.29)\\
(E - QHQ)Q|\psi\rangle &= QHP|\psi\rangle, && (2.30)\\
Q|\psi\rangle &= (E - QHQ)^{-1}QHP|\psi\rangle. && (2.31)
\end{aligned}$$

Substituting (2.31) into (2.26), and exploiting the idempotence of Q, gives:

$$PHP|\psi\rangle + PHQ(E - QHQ)^{-1}QHP|\psi\rangle = EP|\psi\rangle, \quad (2.32)$$

which is of the desired form (2.22) with

$$H_E = PHQ(E - QHQ)^{-1}QHP. \quad (2.33)$$

We now determine the magnitude of H_E acting on the double-well ground state $|\psi_I\rangle$. This magnitude quantifies the error that arises from using the reduced Hamiltonian PHP instead of the full double-well Hamiltonian. Writing $|\psi_I\rangle$ as a linear combination of localized basis states:

$$|\psi_I\rangle = \sum_{i\in\mathcal{S}} a_i|\psi_i\rangle + \sum_{i\notin\mathcal{S}} a_i|\psi_i\rangle, \quad (2.34)$$

we calculate the error estimate $\langle\psi_I|H_E|\psi_I\rangle$ in terms of E_I, $\{a_i\}$, and the elements of H:

$$\begin{aligned}
\langle\psi_I|H_E|\psi_I\rangle &= \langle\psi_I|PHQ(E-QHQ)^{-1}QHP|\psi_I\rangle && (2.35)\\
&= \langle\psi_I|PHQ(E-QHQ)^{-1}QH\left[\sum_{i\in\mathcal{S}} a_iP|\psi_i\rangle + \sum_{i\notin\mathcal{S}} a_iP|\psi_i\rangle\right] && (2.36)\\
&= \langle\psi_I|PHQ(E-QHQ)^{-1}Q\sum_{jk} H_{jk}|\psi_j\rangle\langle\psi_k|\sum_{i\in\mathcal{S}} a_i|\psi_i\rangle && (2.37)\\
&= \langle\psi_I|PHQ(E-QHQ)^{-1}Q\sum_{j}\sum_{i\in\mathcal{S}} a_iH_{ji}|\psi_j\rangle && (2.38)\\
&= \langle\psi_I|PHQ(E-QHQ)^{-1}\sum_{j\notin\mathcal{S}}\sum_{i\in\mathcal{S}} a_iH_{ji}|\psi_j\rangle. && (2.39)
\end{aligned}$$

Note that we cannot invert $(E_I - QHQ)$ without more specific knowledge about the potential. However, we can approximate $(E_I - QHQ)$ as $(E_I - QH^{(S)}Q)$, replacing the full Hamiltonian with the single-well Hamiltonian derived in Section 2.3, as their eigenvalues and eigenvectors are the same to leading order in $\|H^{(T)}\|/\|H^{(S)}\|$. The operator $(E_I - QH^{(S)}Q)$ is diagonal in the localized basis, allowing us to invert it by simply taking the reciprocals of

the eigenvalues:

$$\begin{aligned}
\langle\psi_I|H_E|\psi_I\rangle &\approx \langle\psi_I|PHQ(E_I - QH^{(S)}Q)^{-1}\sum_{j\notin\mathcal{S}}\sum_{i\in\mathcal{S}} a_i H_{ji}|\psi_j\rangle && (2.40)\\
&= \langle\psi_I|PHQ\sum_{k\notin\mathcal{S}}\frac{1}{E_I - H^{(S)}_{kk}}|\psi_k\rangle\langle\psi_k|\sum_{j\notin\mathcal{S}}\sum_{i\in\mathcal{S}} a_i H_{ji}|\psi_j\rangle && (2.41)\\
&= \langle\psi_I|PHQ\sum_{j\notin\mathcal{S}}\sum_{i\in\mathcal{S}}\frac{H_{ji}a_i}{E_I - E_j}|\psi_j\rangle && (2.42)\\
&= \langle\psi_I|P\sum_{kl} H_{kl}|\psi_k\rangle\langle\psi_l|\sum_{j\notin\mathcal{S}}\sum_{i\in\mathcal{S}}\frac{H_{ji}a_i}{E_I - E_j}|\psi_j\rangle && (2.43)\\
&= \langle\psi_I|P\sum_{k}\sum_{j\notin\mathcal{S}}\sum_{i\in\mathcal{S}}\frac{H_{kj}H_{ji}a_i}{E_I - E_j}|\psi_k\rangle && (2.44)\\
&= \left[\sum_{l\in\mathcal{S}}\langle\psi_l|a_l^* + \sum_{l\notin\mathcal{S}}\langle\psi_l|a_l^*\right]P\sum_{k}\sum_{j\notin\mathcal{S}}\sum_{i\in\mathcal{S}}\frac{H_{kj}H_{ji}a_i}{E_I - E_j}|\psi_k\rangle && (2.45)\\
&= \sum_{l\in\mathcal{S}} a_l^*\langle\psi_l|\sum_{k}\sum_{j\notin\mathcal{S}}\sum_{i\in\mathcal{S}}\frac{H_{kj}H_{ji}a_i}{E_I - E_j}|\psi_k\rangle && (2.46)\\
&= \sum_{i\in\mathcal{S}}\sum_{j\notin\mathcal{S}}\sum_{k\in\mathcal{S}}\frac{a_k^* H_{kj}H_{ji}a_i}{E_I - E_j}. && (2.47)
\end{aligned}$$

The denominator of (2.47) corresponds to the energy difference between the double-well ground state and excited states not in $\mathcal{S}$. This energy difference will be at least as large as the single well energy spacing Δ and will be larger for higher excited states. The approximation error is therefore suppressed by a factor of at least $1/\Delta$. The terms H_{kj} and H_{ji} in the numerator represent coupling from states in the reduced subspace $\mathcal{S}$ to higher excited states, due to tunneling. Thus, as tunneling becomes weaker, the numerator is suppressed, as we would expect. The terms a_k and a_i represent the overlap between the low-energy localized states and the low-energy double-well states. These terms will always be less than 1 and of order unity, and thus do not significantly affect the error estimate. Also note that the resonance condition (2.14) implies that the energy separation between E_I and E_{II} is much smaller than Δ, and the error estimate therefore also holds for $|\psi_{II}\rangle$ or any state in

span$\{|\psi_I\rangle, |\psi_{II}\rangle\}$. Due to the low-energy condition (2.17), the state of the system is very likely to be in this subspace, and the error estimate is valid for all of the states we will consider.

We now write the reduced Hamiltonian explicitly, starting from the Hamiltonian for the most general two-state system, and making several simplifications. The Hamiltonian for a two-state system is a Hermitian 2×2 matrix. Any such matrix can be written as:

$$H_2 = c_I I + c_x \sigma_x + c_y \sigma_y + c_z \sigma_z, \tag{2.48}$$

where the σ operators are the standard 2 by 2 Pauli matrices. Their coefficients are given by:

$$c_I = \frac{1}{2}\left(\langle\psi_L|H|\psi_L\rangle + \langle\psi_R|H|\psi_R\rangle\right), \tag{2.49}$$

$$c_x = \frac{1}{2}\left(\langle\psi_L|H|\psi_R\rangle + \langle\psi_R|H|\psi_L\rangle\right), \tag{2.50}$$

$$c_y = \frac{i}{2}\left(\langle\psi_L|H|\psi_R\rangle - \langle\psi_R|H|\psi_L\rangle\right), \tag{2.51}$$

$$c_z = \frac{1}{2}\left(\langle\psi_L|H|\psi_L\rangle - \langle\psi_R|H|\psi_R\rangle\right). \tag{2.52}$$

In most cases, the c_I component can be ignored because it represents a constant energy offset, which has no effect on the dynamics of the reduced Hamiltonian. However, we will occasionally include the c_I component when we discuss the absolute energy levels of the reduced Hamiltonian:

$$c_I = \frac{1}{2}(E_I + E_{II}). \tag{2.53}$$

We know that H is Hermitian and that $|\psi_L\rangle$ and $|\psi_R\rangle$ have real-valued wavefunctions,

which allows us to deduce from (2.51) that

$$c_y \;=\; 0. \tag{2.54}$$

The other off-diagonal component, c_x describes the strength of the coupling between $|\psi_L\rangle$ and $|\psi_R\rangle$ so we define the *tunnel coupling* parameter t by the equation:

$$c_x = \langle\psi_L|H|\psi_R\rangle \;\equiv\; \frac{t}{2}. \tag{2.55}$$

Note that the exact value of t depends on the orthonormalization procedure used to construct $|\psi_L\rangle$ and $|\psi_R\rangle$. However, since these states are created from already near-orthogonal states, the variability of t will be small. We can now quantify the strength of tunneling in terms of t. Specifically, $t \to 0$ represents the limit of an infinite barrier with no tunneling.

The c_z component can be easily calculated in the weak tunneling limit:

$$\begin{aligned}
\frac{1}{2}\left(\langle\psi_L|H|\psi_L\rangle - \langle\psi_R|H|\psi_R\rangle\right) \;&\to\; \frac{1}{2}\left(\langle\psi_L|H^{(S)}|\psi_L\rangle - \langle\psi_R|H^{(S)}|\psi_R\rangle\right) && (2.56)\\
&= \frac{1}{2}(E_L - E_R) && (2.57)\\
&= \frac{\epsilon}{2}. && (2.58)
\end{aligned}$$

In other words, c_z is proportional to the detuning in the limit of weak tunneling. In the finite tunneling case we could write c_z more generally as:

$$c_z \;=\; \frac{\epsilon + \gamma(\epsilon)}{2}, \tag{2.59}$$

where $\gamma(\epsilon)$ represents the deviation of c_z from its assumed value. In practice however, $\gamma(\epsilon)$ is usually assumed to be zero.

We may now combine (2.53), (2.54), (2.55), and (2.59) to give the form of the reduced

Hamiltonian H_2:

$$H_2 = \frac{E_I + E_{II}}{2} + \begin{bmatrix} \epsilon/2 & t/2 \\ t/2 & -\epsilon/2 \end{bmatrix}. \tag{2.60}$$

2.5 Spectrum of the reduced Hamiltonian

The reduced Hamiltonian is a 2 by 2 matrix, so its exact eigenvalues can be found easily. The characteristic equation for H_2 (excluding the identity component) is:

$$\left(\frac{\epsilon}{2} - \lambda\right)\left(-\frac{\epsilon}{2} - \lambda\right) - \left(\frac{t}{2}\right)^2 = 0. \tag{2.61}$$

Solving the above for λ gives two solutions:

$$\lambda_\pm = \pm\frac{1}{2}\sqrt{\epsilon^2 + t^2}. \tag{2.62}$$

The difference between the two eigenvalues $\lambda_\pm$ gives the *tunnel splitting* δ between the double-well eigenstates, $|\psi_I\rangle$ and $|\psi_{II}\rangle$:

$$\delta = \sqrt{\epsilon^2 + t^2}. \tag{2.63}$$

When $\epsilon \gg t$, the tunnel splitting can be approximated to second order in t/ϵ:

$$\delta \approx \epsilon + \frac{t^2}{2\epsilon}. \tag{2.64}$$

Equations (2.63) and (2.64) provide an important connection between the detuning, tunnel coupling, and tunnel splitting. However, the derivation of this connection involved neglecting coupling to higher excited states by projecting onto a low-energy, localized subspace.

It is therefore necessary to determine when the error (2.47) induced by this approximation is less than the value we are trying to calculate. The value we are most concerned with is the change in the tunnel splitting due to tunneling, or $\delta - \epsilon$. We therefore want:

$$\delta - \epsilon \gg \sum_{i\in\mathcal{S}}\sum_{j\notin\mathcal{S}}\sum_{k\in\mathcal{S}} \frac{a_k H_{kj} H_{ji} a_i}{E_I - E_j}. \tag{2.65}$$

We can nondimensionalize the above equation using the tunnel coupling and the single-well level spacing Δ to get

$$\delta - \epsilon \gg \frac{t^2}{\Delta} C, \tag{2.66}$$

$$C = \sum_{i\in\mathcal{S}}\sum_{j\notin\mathcal{S}}\sum_{k\in\mathcal{S}} \left(\frac{a_k H_{kj} H_{ji} a_i}{t^2}\right)\left(\frac{\Delta}{E_I - E_j}\right), \tag{2.67}$$

where C is some numerical value depending on the properties of the double-well potential. When $t \ll \epsilon$ we can substitute in (2.64), yielding:

$$\frac{t^2}{2\epsilon} \gg \frac{t^2}{\Delta} C, \tag{2.68}$$

$$\epsilon \ll \frac{\Delta}{2C}. \tag{2.69}$$

In other words, the effects of higher excited states are suppressed as the detuning becomes much smaller than the single-well level spacing. However, since we do not know the value of C, we cannot say precisely how small the detuning must be. Also, there is a minimum detuning below which (2.64) breaks down, so the effects of tunneling to higher excited states must be considered as a possible contribution in all cases.

To this point, we have considered ϵ and t to be constants depending only on the potentials $V(x)$. However, in the following chapters, we consider not just one potential, but a family of potentials $V_\epsilon(x)$ parameterized by their detuning. In this case, all matrix elements, including

t, *could potentially be dependent functions of* ϵ. The theoretical motivation and numerical determination of this dependence of t on ϵ is the primary focus of the work described in this thesis.

Chapter 3

WKB Energy Quantization

In the previous chapter, we saw that the tunnel coupling of a double-well can be determined from the detuning (a known quantity) and the tunnel splitting. The problem at hand is thus how to determine the splitting between the lowest two levels in a double-well. If an exact solution to the Schrödinger equation was known for the given potential, the tunnel splitting could be easily calculated from the energy levels. However, exact solutions are not known for most types of double-well potentials. Instead, we use the Wentzel-Kramers-Brillouin (WKB) approximation to determine the approximate energy levels, and thus the tunnel splitting. The WKB approximation provides approximate, analytic expressions for the wave functions and energy levels for many potentials that have no known exact solutions. WKB is thus well suited for deriving an approximate equation relating the tunnel coupling to the detuning.

3.1 The WKB approximation

Fundamentally, the WKB approximation is a technique for simplifying differential equations using a number of assumptions [3]. In the context of quantum mechanics, the WKB method can be used to simplify the Schrödinger equation [13, 17]. The one-dimensional Schrödinger

equation for a particle of mass m in a potential $V(x)$ is:

$$-\frac{\hbar^2}{2m}\frac{d^2}{dx^2}\psi(x) + V(x)\psi(x) \;=\; E\psi(x). \tag{3.1}$$

If we nondimensionalize the position as $x = l_0 z$, where l_0 is a characteristic length, and z is dimensionless, we can rearrange the Schrödinger equation to give:

$$-\left[\frac{\hbar}{l_0\sqrt{2m(E-\tilde{V}(z))}}\right]^2 \frac{d^2}{dz^2}\tilde{\psi}(z) \;=\; \tilde{\psi}(z), \tag{3.2}$$

where $\tilde{\psi}(z) = \psi(x)$ and $\tilde{V}(z) = V(x)$.

Let us consider the bracketed, dimensionless term in (3.2). In classically allowed regions, where $E > V(x)$, the radical appearing in the denominator represents the momentum of a classical particle, so we define:

$$p(x, E) \;=\; \sqrt{2m|E - V(x)|}, \tag{3.3}$$

where we have taken the absolute value of $E - V(x)$ in order to include the classically forbidden regions where $E < V(x)$. The denominator is thus $l_0 p(x, E)$, with dimensions of action. For approximately classical systems, the action is large with respect to $\hbar$, and the bracketed term will be a small parameter. In fact, the WKB approximation relies on this assumption, known as the *semi-classical approximation*:

$$l_0\sqrt{2m|E - V(x)|} \;\gg\; \hbar. \tag{3.4}$$

Continuing from the semi-classical approximation, the derivation of the WKB method (given in [3]) makes an additional assumption. Depending on the sign of $E - V(x)$, we assume that either the amplitude or phase of the wave function varies slowly. The amplitude

must vary slowly in the classically allowed region, while the phase must vary slowly in the classically forbidden region. However, these assumptions cannot be satisfied near the *classical turning points*, where $E = V(x)$.

3.1.1 WKB solutions

Note that the Schrödinger equation is a second-order differential equation, so we should expect two independent solutions. Indeed, WKB yields two independent solutions for the wave function. In general, valid wave functions can be linear combinations of these two WKB basis solutions. However, the basis solutions take different forms in the allowed and forbidden regions, and are not valid near the classical turning points.

The WKB solutions in a given region are always written relative to one of the turning points bordering that region. In the classically allowed regions, the two WKB basis solutions are:

$$\psi(x) = \frac{A}{\sqrt{p(x,E)}} \sin\left[\frac{1}{\hbar}\int_{x_0}^{x} p(x',E)dx' + \frac{\pi}{4}\right], \tag{3.5}$$

$$\psi(x) = \frac{B}{\sqrt{p(x,E)}} \sin\left[\frac{1}{\hbar}\int_{x_0}^{x} p(x',E)dx' - \frac{\pi}{4}\right], \tag{3.6}$$

where x_0 is the turning point, and A and B are normalization constants with dimensions of $[M^{1/2}T^{-1/2}]$. In the forbidden region, the WKB basis solutions are:

$$\psi(x) = \frac{C}{\sqrt{p(x,E)}} \exp\left[+\frac{1}{\hbar}\int_{x}^{x_0} p(x',E)dx'\right], \tag{3.7}$$

$$\psi(x) = \frac{D}{\sqrt{p(x,E)}} \exp\left[-\frac{1}{\hbar}\int_{x}^{x_0} p(x',E)dx'\right], \tag{3.8}$$

where C and D are normalization constants with dimensions $[M^{1/2}T^{-1/2}]$. In the classically allowed regions, the WKB solutions thus exhibit oscillatory behavior, while in the forbidden

regions, they exhibit exponential decay and/or growth.

3.1.2 Connection formulas

Although the WKB basis solutions have different forms in different regions, the solutions in different region cannot all be independent of each other. As mentioned previously, there are two independent solutions of the full Schrödinger equation, i.e. two degrees of freedom. One of these degrees of freedom is removed by normalization. Thus, fixing the WKB wave function in one region determines the wave function in every other region. The basis solution amplitudes in different regions are related by the WKB *connection formulas*.

The connection formulas relate the amplitudes of the WKB solution on one side of a turning point to those of the solution on the other side of the turning point. For a turning point x_0 with a forbidden region on the left and an allowed region on the right, the connection formulas are:

$$\frac{A}{\sqrt{p(x,E)}}\exp\left[-\frac{1}{\hbar}\int_x^{x_0} p(x',E)dx'\right] \quad \Leftrightarrow \quad \frac{2A}{\sqrt{p(x,E)}}\sin\left[\frac{1}{\hbar}\int_{x_0}^{x} p(x',E)dx' + \frac{\pi}{4}\right], \quad (3.9)$$

$$\frac{B}{\sqrt{p(x,E)}}\exp\left[+\frac{1}{\hbar}\int_x^{x_0} p(x',E)dx'\right] \quad \Leftrightarrow \quad \frac{B}{\sqrt{p(x,E)}}\sin\left[\frac{1}{\hbar}\int_{x_0}^{x} p(x',E)dx' - \frac{\pi}{4}\right], \quad (3.10)$$

where the arrows signify that the given basis solutions in the forbidden region correspond to the given basis solutions in the allowed region, with the same amplitude, and vice versa. Note that the factor of 2 between (3.10) and (3.9) occurs due to the different asymptotic behavior of growing and decaying Airy functions, which arise in the derivation. Connection formulas can also be written for the case of an allowed region on the left and a forbidden

region on the right:

$$\frac{A}{\sqrt{p(x,E)}}\exp\left[-\frac{1}{\hbar}\int_{x_0}^{x}p(x',E)dx'\right] \;\Leftrightarrow\; \frac{2A}{\sqrt{p(x,E)}}\sin\left[\frac{1}{\hbar}\int_{x}^{x_0}p(x',E)dx'+\frac{\pi}{4}\right], \quad (3.11)$$

$$\frac{B}{\sqrt{p(x,E)}}\exp\left[+\frac{1}{\hbar}\int_{x_0}^{x}p(x',E)dx'\right] \;\Leftrightarrow\; \frac{B}{\sqrt{p(x,E)}}\sin\left[\frac{1}{\hbar}\int_{x}^{x_0}p(x',E)dx'-\frac{\pi}{4}\right]. \quad (3.12)$$

The WKB solutions and connection formulas all depend on similar integrals of the momentum. We thus define the WKB *phase integral* $\theta_{ab}(E)$ to be:

$$\theta_{ab}(E) \;=\; \frac{1}{\hbar}\int_{a}^{b}p(x,E)\,dx. \quad (3.13)$$

These phase integrals are monotonically increasing functions of energy, and play an important role in WKB energy quantization.

3.2 Single-well quantization

By applying the connection formulas (3.9), (3.10), (3.11), and (3.12) at each turning point and imposing boundary conditions, WKB can be used to derive a quantization condition for the allowed energies of a potential. We first review the case of a single-well potential with only one classically allowed region.

We divide the well into three regions (see Figure 3.1). Regions I and III are classically forbidden, while Region II is classically allowed. In Region I, the wave function must vanish as $x \to -\infty$, so the only WKB solution with nonzero amplitude is (3.8) which decays as x moves away from the turning point. Applying the connection formula (3.9) at x_1 gives an expression for the wave function in the allowed region:

$$\psi_1(x) \;=\; \frac{2A}{\sqrt{p(x)}}\sin\left[\frac{1}{\hbar}\int_{x_1}^{x}p(x')dx'+\frac{\pi}{4}\right]. \quad (3.14)$$

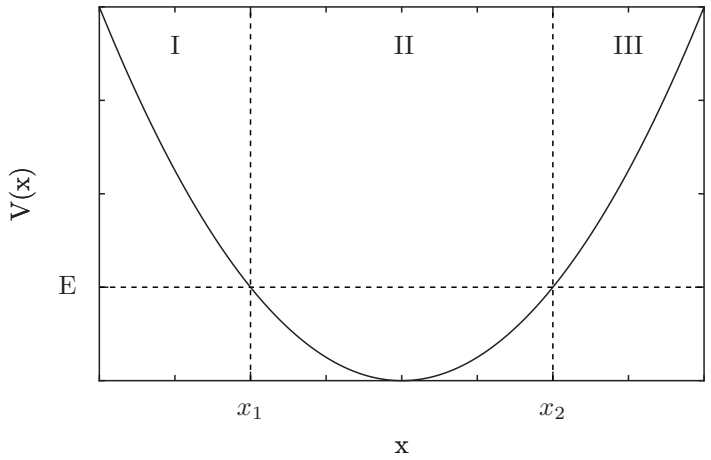

Figure 3.1: Schematic diagram of a single-well potential with two forbidden regions (I,III) and one allowed region (II).

Similarly, only the exponentially decaying solution is present in Region III, so applying the connection formula (3.11) at x_2 gives another expression for the wave function in the allowed region:

$$\psi_2(x) = \frac{2B}{\sqrt{p(x)}} \sin\left[\frac{1}{\hbar}\int_x^{x_2} p(x')dx' + \frac{\pi}{4}\right]. \tag{3.15}$$

Since both $\psi_1(x)$ and $\psi_2(x)$ are solutions for Region II, they must be equal:

$$\frac{2A}{\sqrt{p(x)}} \sin\left[\frac{1}{\hbar}\int_{x_1}^{x} p(x')dx' + \frac{\pi}{4}\right] = \frac{2B}{\sqrt{p(x)}} \sin\left[\frac{1}{\hbar}\int_x^{x_2} p(x')dx' + \frac{\pi}{4}\right]. \tag{3.16}$$

A -1 can be factored out of the argument of either sine term, for instance:

$$\frac{2A}{\sqrt{p(x)}} \sin\left[\frac{1}{\hbar}\int_{x_1}^{x} p(x')dx' + \frac{\pi}{4}\right] = -\frac{2B}{\sqrt{p(x)}} \sin\left[-\frac{1}{\hbar}\int_x^{x_2} p(x')dx' - \frac{\pi}{4}\right]. \tag{3.17}$$

For Equation (3.17) to be satisifed, the amplitudes of each side must have the same magni-

tude, and the phases must be the same modulo π:

$$|A| = |B| \tag{3.18}$$

$$\frac{1}{\hbar}\int_{x_1}^{x} p(x')dx' + \frac{\pi}{4} = -\frac{1}{\hbar}\int_{x}^{x_2} p(x')dx' - \frac{\pi}{4} + n\pi, \tag{3.19}$$

which simplifies to

$$\frac{1}{\hbar}\int_{x_1}^{x} p(x')dx' + \frac{1}{\hbar}\int_{x}^{x_2} p(x')dx' = n\pi - \frac{\pi}{2}. \tag{3.20}$$

Combining the integrals gives the WKB quantization condition for a single-well:

$$\theta_{12} \equiv \frac{1}{\hbar}\int_{x_1}^{x_2} p(x)dx = n\pi - \frac{\pi}{2}. \tag{3.21}$$

3.2.1 Application to harmonic oscillator

We now review a simple example, applying the single-well quantization condition (3.21) to a one-dimensional harmonic oscillator [13]. For the harmonic oscillator, the phase integral is given by:

$$\theta_{12} = \frac{1}{\hbar}\int_{x_1}^{x_2} \sqrt{2m[E - V(x)]}dx \tag{3.22}$$

$$V(x) = \frac{m\omega^2}{2}(x - x_0)^2 \tag{3.23}$$

$$x_1 = x_0 - \frac{1}{\omega}\sqrt{\frac{2E}{m}} \tag{3.24}$$

$$x_2 = x_0 + \frac{1}{\omega}\sqrt{\frac{2E}{m}}. \tag{3.25}$$

Letting $y = x - x_0$, the integral becomes

$$\theta_{12} = \frac{1}{\hbar}\int_{y_1}^{y_2}\sqrt{2m\left[E - \frac{m\omega^2}{2}y^2\right]}dy \tag{3.26}$$

$$= \frac{\sqrt{2mE}}{\hbar}\int_{y_1}^{y_2}\sqrt{1 - \frac{m\omega^2}{2E}y^2}dy. \tag{3.27}$$

Letting $z = \omega\sqrt{\frac{m}{2E}}y$, and exploiting the even symmetry of the potential, the integral becomes

$$\theta_{12} = \frac{2E}{\hbar\omega}\int_{z_1}^{z_2}\sqrt{1 - z^2}dz \tag{3.28}$$

$$= \frac{4E}{\hbar\omega}\int_{0}^{z_2}\sqrt{1 - z^2}dz \tag{3.29}$$

$$= \frac{2E}{\hbar\omega}\left[z\sqrt{1 - z^2} + \sin^{-1}(z)\right]_0^{z_2}. \tag{3.30}$$

Calculating z_2 from (3.25) gives

$$z_2 = \omega\sqrt{\frac{m}{2E}}\left[\left(x_0 + \frac{1}{\omega}\sqrt{\frac{2E}{m}}\right) - x_0\right] = 1. \tag{3.31}$$

Thus evaluating the phase integral gives

$$\theta_{12} = \frac{2E}{\hbar\omega}\left[z\sqrt{1 - z^2} + \sin^{-1}(z)\right]_0^1 \tag{3.32}$$

$$= \frac{E\pi}{\hbar\omega}. \tag{3.33}$$

Combining the phase integral (3.33) with the single-well quantization condition (3.21) gives the WKB energy levels for the harmonic oscillator, which in this case happen to be the same as the energy levels from the exact solution:

$$E = \hbar\omega\left(n - \frac{1}{2}\right). \tag{3.34}$$

3.3 Double-well quantization

The same WKB quantization scheme may be applied to a double-well, illustrated schematically in Figure (3.2).

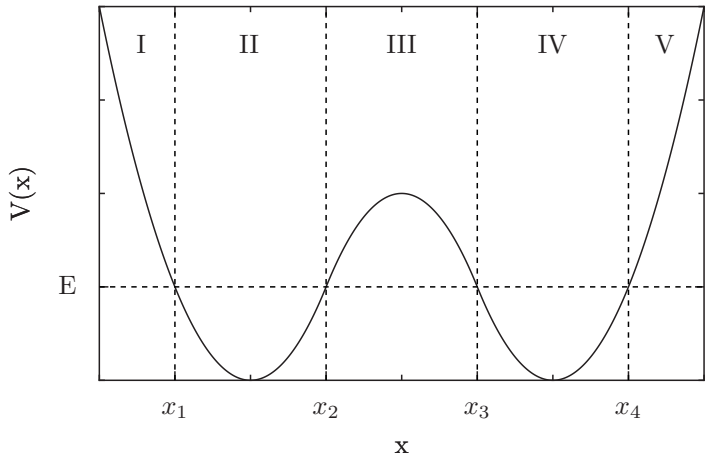

Figure 3.2: Schematic diagram of a double-well potential with three forbidden regions (I,III,V) and two allowed regions (II,IV).

We begin by deriving a quantization condition for Region II analogous to Equation (3.21). Again, applying the boundary condition for Region I leaves only the exponentially growing solution. Applying the connection formula at x_1 then gives an expression for the wave function in Region II:

$$\psi_1(x) \;=\; \frac{2A}{\sqrt{\sqrt{p(x)}}} \sin\left[\frac{1}{\hbar}\int_{x_1}^{x} p(x')dx' + \frac{\pi}{4}\right]. \tag{3.35}$$

However, the solution in Region III must have both growing and decaying solutions present. Considering the Region III solutions in terms of x_2 and letting B_L and C_L be the amplitudes of the decaying and growing solutions respectively, the connection formulas give another

expression for the wave function in region II:

$$\psi_2(x) = \frac{2B_L}{\sqrt{\sqrt{p(x)}}} \sin\left[\frac{1}{\hbar}\int_x^{x_2} p(x')dx' + \frac{\pi}{4}\right] + \frac{C_L}{\sqrt{\sqrt{p(x)}}} \sin\left[\frac{1}{\hbar}\int_x^{x_2} p(x')dx' - \frac{\pi}{4}\right] \quad (3.36)$$

$$= \frac{2B_L}{\sqrt{p(x')}} \cos\theta + \frac{C_L}{\sqrt{p(x')}} \sin\theta \quad (3.37)$$

$$\theta = \frac{1}{\hbar}\int_x^{x2} p(x')dx' - \frac{\pi}{4}. \quad (3.38)$$

As in Section 3.2, we equate the two expressions (3.35, 3.37) for the wave function in Region II and cancel common factors giving

$$2A \sin\left[\frac{1}{\hbar}\int_{x_1}^{x} p(x')dx' + \frac{\pi}{4}\right] = 2B_L \cos\theta + C_L \sin\theta. \quad (3.39)$$

Using trigonometric identities to simplify the right hand side, gives

$$2A \sin\left[\frac{1}{\hbar}\int_{x_1}^{x} p(x')dx' + \frac{\pi}{4}\right] = \sqrt{4B_L^2 + C_L^2} \sin\left(\theta + \frac{\pi}{2} - \phi_L\right) \quad (3.40)$$

$$\phi_L = \cos^{-1}\left[\frac{2B_L}{\sqrt{4B_L^2 + C_L^2}}\right]. \quad (3.41)$$

As in Section 3.2, the magnitude of the sines must be equal, and the magnitude of the phases must be equal modulo π:

$$4A^2 = 4B_L^2 + C_L^2 \quad (3.42)$$

$$\frac{1}{\hbar}\int_{x_1}^{x} p(x')dx' + \frac{\pi}{4} = -\frac{1}{\hbar}\int_x^{x2} p(x')dx' + \frac{3\pi}{4} + \phi_L + n\pi. \quad (3.43)$$

Simplifying and combining the integrals gives the the quantization condition for Region II:

$$\theta_{12} \equiv \frac{1}{\hbar}\int_{x_1}^{x_2} p(x)dx = \pi\left(n - \frac{1}{2}\right) + \phi_L. \quad (3.44)$$

A similar treatment for the turning point x_3 yields the condition for Region IV:

$$\theta_{34} \equiv \frac{1}{\hbar}\int_{x_3}^{x_4} p(x)dx \;=\; \pi\left(m-\frac{1}{2}\right)+\phi_R, \tag{3.45}$$

with $m = 1, 2, \ldots$ and ϕ_R given by

$$\phi_R \;=\; \cos^{-1}\left[\frac{2C_R}{\sqrt{4C_R^2+B_R^2}}\right], \tag{3.46}$$

where B_R and C_R are the amplitudes of the decaying and growing Region III solutions in terms of x_3.

We now have the quantization conditions (3.44, 3.45) for Regions II and IV, but they contain the free parameters ϕ_L and ϕ_R. To eliminate these free parameters, we consider the WKB solution in Region III. The coefficients B_L, C_L, B_R, C_R define two expressions for solution, which must be equal:

$$\psi_{III} \;=\; \frac{B_L}{\sqrt{p(x')}}\exp\left[-\frac{1}{\hbar}\int_{x_2}^{x} p(x')dx'\right]+\frac{C_L}{\sqrt{p(x')}}\exp\left[+\frac{1}{\hbar}\int_{x_2}^{x} p(x')dx'\right] \tag{3.47}$$

$$\;=\; \frac{B_R}{\sqrt{p(x')}}\exp\left[+\frac{1}{\hbar}\int_{x}^{x_3} p(x')dx'\right]+\frac{C_R}{\sqrt{p(x')}}\exp\left[-\frac{1}{\hbar}\int_{x}^{x_3} p(x')dx'\right]. \tag{3.48}$$

Equations (3.47) and (3.48) each contain a term that grows exponentially with x and a term that decays exponentially with x. Equating the growing terms from each equation and the decaying term from each equation gives two constraints:

$$B_L\exp\left[-\frac{1}{\hbar}\int_{x_2}^{x} p(x')dx'\right] \;=\; B_R\exp\left[\frac{1}{\hbar}\int_{x}^{x_3} p(x')dx'\right] \tag{3.49}$$

$$C_L\exp\left[\frac{1}{\hbar}\int_{x_2}^{x} p(x')dx'\right] \;=\; C_R\exp\left[-\frac{1}{\hbar}\int_{x}^{x_3} p(x')dx'\right]. \tag{3.50}$$

Combining the integrals in these constraints gives

$$\frac{B_L}{B_R} = \frac{C_R}{C_L} = \exp\theta_{23} \tag{3.51}$$

$$\theta_{23} \equiv \frac{1}{\hbar}\int_{x_2}^{x_3} p(x)dx. \tag{3.52}$$

The constraints (3.44, 3.45, 3.51) may be combined to give a single quantization condition for the allowed WKB energies for a double-well. Applying trigonometric identities to (3.41) and (3.46), and plugging in (3.51) gives

$$\tan\phi_L \tan\phi_R = \left(\frac{C_L}{2B_L}\right)\left(\frac{B_R}{2C_R}\right) \tag{3.53}$$

$$= \frac{1}{4}\exp\left(-2\theta_{23}\right). \tag{3.54}$$

Equation (3.54) may combined with Equations (3.44) and (3.45) to give the WKB quantization condition for a double-well in terms of the phase integrals θ_{12} and θ_{34}:

$$\cot\theta_{12}\cot\theta_{34} = \frac{1}{4}\exp\left(-2\theta_{23}\right), \tag{3.55}$$

confirming the results given in [23] and [20].

Equation (3.55) is a nonlinear constraint approximately determining the allowed energy levels of a double-well potential. In the chapters that follow, this equation allows us to determine expressions for the energy levels a double-well, and thus the tunnel coupling.

Chapter 4

Tunnel Coupling From WKB

The WKB approximation discussed in the previous chapter can be used to determine the tunnel coupling of a quantum double well, as well as the dependence of the tunnel coupling on detuning. The WKB quantization condition (3.55) describes the allowed energy levels in a 1-D quantum double well. The allowed energy levels in turn determine the tunnel splitting, and therefore the tunnel coupling through the relation (2.63). We derive an expression for the tunnel coupling as a function of detuning by using WKB to determine a general expression for the tunnel coupling of a family of potentials $V_\epsilon(x)$, parameterized by their detuning. We then discuss the detuning-dependence this result implies for various potentials.

We begin in Section 4.1 by formally defining a general double-well potential in terms of parameters relevant to our analysis. We derive a general expression for tunnel coupling in terms of these parameters in Section 4.2, and discuss the implications of the expression for several types of potentials in Section 4.3.

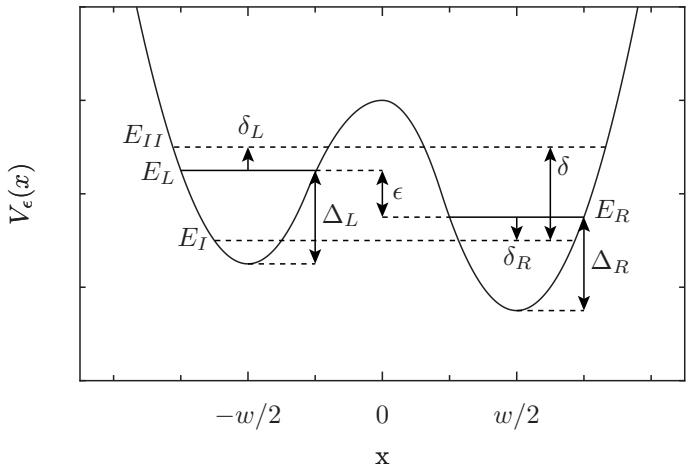

Figure 4.1: Schematic diagram of a family of double-well potential. E_L and E_R are the single well energies, offset from the potential minima by Δ_L and Δ_R respectively. ϵ is the offset between left and right single-well energies, and defines the potential by shifting the wells rigidly up or down. E_I and E_{II} are the lowest two double-well energies, differing from the single-well energies by the shifts δ_R and δ_L respectively.

4.1 Parameters of the potential

There are many possible shapes for a double well potential, but the properties relevant to our analysis can be specified succinctly by a few parameters (Figure 4.1). As in Section 2.1, we analyze the double-well in terms of two isolated single-wells $V_L(x)$ and $V_R(x)$ with minima:

$$V_L(0) = V_R(0) = 0. \tag{4.1}$$

The WKB single-well quantization condition (3.21) predicts the ground state energies for each well. However, adding any constant offset to the potentials will add the same offset to their corresponding ground state energies, so the absolute ground state energy is not particularly meaningful. Instead, we define the energy offsets, Δ_L and Δ_R, as the difference between the minimum of each potential and its ground state energy. These offsets depend only on the shape of the single-well potentials, independent of any constant energy offset.

The family of double-well potentials $V_\epsilon(x)$ is constructed from the single-well potentials

$V_L(x)$ and $V_R(x)$. As in Section 2.1, $V_\epsilon(x)$ has the shape of $V_L(x)$ for negative x and the shape of $V_R(x)$ for positive x. However, we now add a constant offset to each potential:

$$V_\epsilon(x) = \begin{cases} V_L(x + w/2) + \frac{\Delta_R - \Delta_L}{2} + \frac{\epsilon}{2} & \text{if } x < 0, \\ V_R(x - w/2) - \frac{\Delta_R - \Delta_L}{2} - \frac{\epsilon}{2} & \text{if } x > 0, \end{cases} \tag{4.2}$$

where w is the minimum-to-minimum width of the double-well potential, and ϵ is the detuning. Having shifted $V_L(x)$ and $V_R(x)$ each by a constant energy, their ground states will also be shifted by the same amount. We define these shifted single-well energies $E_L(\epsilon)$ and $E_R(\epsilon)$ as:

$$E_L(\epsilon) \equiv \Delta_L + \frac{\Delta_R - \Delta_L}{2} + \frac{\epsilon}{2} \tag{4.3}$$

$$= \frac{\Delta_R + \Delta_L}{2} + \frac{\epsilon}{2}, \tag{4.4}$$

$$E_R(\epsilon) \equiv \Delta_R - \frac{\Delta_R - \Delta_L}{2} - \frac{\epsilon}{2} \tag{4.5}$$

$$= \frac{\Delta_L + \Delta_R}{2} - \frac{\epsilon}{2}. \tag{4.6}$$

Note that the difference between these energies is given by:

$$E_L(\epsilon) - E_R(\epsilon) = \left(\Delta_L + \frac{\Delta_R - \Delta_L}{2} + \frac{\epsilon}{2}\right) - \left(\Delta_R - \frac{\Delta_R - \Delta_L}{2} - \frac{\epsilon}{2}\right) \tag{4.7}$$

$$= \Delta_L - \Delta_R + \Delta_R - \Delta_L + \epsilon \tag{4.8}$$

$$= \epsilon. \tag{4.9}$$

Thus the definition of $V_\epsilon(x)$ has been chosen such that ϵ represents the difference between the left and right single-well energies, in agreement with our earlier conventions.

The remaining parameters concern shifts in energy levels due to tunneling. The single-well energy levels $E_L(\epsilon)$ and $E_R(\epsilon)$ will be shifted by some amounts $\delta_L(\epsilon)$ and $\delta_R(\epsilon)$ respectively,

giving the double-well energy levels E_I and E_{II}:

$$E_I(\epsilon) = E_R(\epsilon) + \delta_R(\epsilon), \tag{4.10}$$

$$E_{II}(\epsilon) = E_L(\epsilon) + \delta_L(\epsilon). \tag{4.11}$$

Note that perturbations tend to lower the ground state, so $\delta_R(\epsilon)$ will be negative. Combining (4.10) and (4.11) with (4.9) gives an expression for the tunnel splitting $\delta(\epsilon)$:

$$\delta(\epsilon) = E_{II}(\epsilon) - E_I(\epsilon) \tag{4.12}$$

$$= E_L(\epsilon) + \delta_L(\epsilon) - E_R(\epsilon) - \delta_R(\epsilon) \tag{4.13}$$

$$= \epsilon + \delta_L(\epsilon) - \delta_R(\epsilon). \tag{4.14}$$

Noting that $\delta_R(\epsilon)$ is negative, the above can be written more clearly as:

$$\delta(\epsilon) = \epsilon + |\delta_L(\epsilon)| + |\delta_R(\epsilon)|. \tag{4.15}$$

Equating (2.63) and (4.15) gives a general expression for the tunnel coupling t:

$$\delta = \sqrt{t^2 + \epsilon^2}, \tag{4.16}$$

$$\epsilon + |\delta_L(\epsilon)| + |\delta_R(\epsilon)| = \sqrt{t^2 + \epsilon^2}, \tag{4.17}$$

$$t(\epsilon) = \sqrt{(\epsilon + |\delta_L(\epsilon)| + |\delta_R(\epsilon)|)^2 - \epsilon^2}. \tag{4.18}$$

In the case of $\epsilon \gg t$ we can use (2.64) instead, giving:

$$\begin{aligned} \delta &\approx \epsilon + \frac{t^2}{2\epsilon}, && (4.19) \\ \epsilon + |\delta_L(\epsilon)| + |\delta_R(\epsilon)| &\approx \epsilon + \frac{t^2}{2\epsilon}, && (4.20) \\ t(\epsilon) &\approx \sqrt{2\epsilon\,(|\delta_L(\epsilon)| + |\delta_R(\epsilon)|)}. && (4.21) \end{aligned}$$

Note that (4.21) is equivalent to (4.18) in the limit $\epsilon \gg t$.

4.2 General expression for tunnel coupling

In the previous section, we derived the connection between the double-well energy levels and the tunnel coupling for a potential $V_\epsilon(x)$ with detuning ϵ. The WKB approximation gives the allowed double-well energy levels through Equation (3.55). We now rewrite (3.55) in terms of the detuning-dependent parameters of $V_\epsilon(x)$:

$$\cot\left(\phi_{12}(E(\epsilon),\epsilon) + \frac{\pi}{2}\right)\cot\left(\phi_{34}(E(\epsilon),\epsilon) + \frac{\pi}{2}\right) = \frac{1}{4}\exp\left[-2\theta(E(\epsilon),\epsilon)\right], \qquad (4.22)$$

with phase integrals and phase shifts:

$$\begin{aligned} \phi_{12}(E(\epsilon),\epsilon) &= \frac{1}{\hbar}\int_{x_1}^{x_2}\sqrt{2m(E(\epsilon) - V_\epsilon(x))}\,dx - \frac{\pi}{2}, && (4.23) \\ \phi_{34}(E(\epsilon),\epsilon) &= \frac{1}{\hbar}\int_{x_3}^{x_4}\sqrt{2m(E(\epsilon) - V_\epsilon(x))}\,dx - \frac{\pi}{2}, && (4.24) \\ \theta_{23}(E(\epsilon),\epsilon) &= \frac{1}{\hbar}\int_{x_2}^{x_3}\sqrt{2m(E(\epsilon) - V_\epsilon(x))}\,dx, && (4.25) \end{aligned}$$

where m is the particle mass, and x_n is the nth classical turning point. Note that the energy E is an implicit function of the detuning because the values of E that solve (4.22) will be different for different values of ϵ.

4.2.1 Detuning-dependence of WKB phase shifts

The WKB phase shifts $\phi_{12}(E(\epsilon),\epsilon)$ and $\phi_{34}(E(\epsilon),\epsilon)$ can be rewritten in a form that distinguishes between the detuning-independent terms (properties of the single-wells) and the detuning-dependent terms (properties of the double-well). We first use Equation (4.2) to rewrite $V_\epsilon(x)$:

$$\phi_{12}(E(\epsilon),\epsilon) = \frac{\sqrt{2m}}{\hbar}\int_{x_1}^{x_2}\sqrt{E(\epsilon)-[V_L(x+w/2)+(\Delta_R-\Delta_L)/2+\epsilon/2]}\,dx-\frac{\pi}{2}, \quad (4.26)$$

$$\phi_{34}(E(\epsilon),\epsilon) = \frac{\sqrt{2m}}{\hbar}\int_{x_3}^{x_4}\sqrt{E(\epsilon)-[V_R(x-w/2)-(\Delta_R-\Delta_L)/2-\epsilon/2]}\,dx-\frac{\pi}{2}, \quad (4.27)$$

Regrouping terms gives:

$$\phi_{12}(E(\epsilon),\epsilon) = \frac{\sqrt{2m}}{\hbar}\int_{x_1}^{x_2}\sqrt{[E(\epsilon)-(\Delta_R-\Delta_L)/2+\epsilon/2]-V_L(x+w/2)}\,dx-\frac{\pi}{2}, \quad (4.28)$$

$$\phi_{34}(E(\epsilon),\epsilon) = \frac{\sqrt{2m}}{\hbar}\int_{x_3}^{x_4}\sqrt{[E(\epsilon)+(\Delta_R-\Delta_L)/2-\epsilon/2]-V_R(x-w/2)}\,dx-\frac{\pi}{2}, \quad (4.29)$$

Combining these equations with the single-well energies (4.3) and (4.6) gives:

$$\phi_{12}(E(\epsilon),\epsilon) = \frac{\sqrt{2m}}{\hbar}\int_{x_1}^{x_2}\sqrt{(E(\epsilon)-E_L(\epsilon))+(\Delta_L-V_L(x+w/2))}\,dx-\frac{\pi}{2}, \quad (4.30)$$

$$\phi_{34}(E(\epsilon),\epsilon) = \frac{\sqrt{2m}}{\hbar}\int_{x_3}^{x_4}\sqrt{(E(\epsilon)-E_R(\epsilon))+(\Delta_R-V_R(x-w/2))}\,dx-\frac{\pi}{2}, \quad (4.31)$$

where the first term in parentheses is the shift in energy from the single-well ground state, and the second term is independent of detuning.

The derivatives of the WKB phase shifts with respect to energy are also necessary for

the derivation of the tunnel coupling:

$$\frac{\partial}{\partial E}\phi_{12}(E(\epsilon),\epsilon) = \frac{\sqrt{2m}}{2\hbar}\int_{x_1}^{x^2}\left[(E(\epsilon)-E_L(\epsilon))+(\Delta_L-V_L(x))\right]^{-1/2}\,dx, \tag{4.32}$$

$$\frac{\partial}{\partial E}\phi_{34}(E(\epsilon),\epsilon) = \frac{\sqrt{2m}}{2\hbar}\int_{x_3}^{x^4}\left[(E(\epsilon)-E_L(\epsilon))+(\Delta_R-V_R(x))\right]^{-1/2}\,dx. \tag{4.33}$$

The value of these derivatives at their corresponding single-well energies is of particular interest:

$$\frac{\partial}{\partial E}\phi_{12}(E_L(\epsilon),\epsilon) = \frac{\sqrt{2m}}{2\hbar}\int_{x_1}^{x^2}(\Delta_L-V_L(x))^{-1/2}\,dx, \tag{4.34}$$

$$\frac{\partial}{\partial E}\phi_{34}(E_R(\epsilon),\epsilon) = \frac{\sqrt{2m}}{2\hbar}\int_{x_3}^{x^4}(\Delta_R-V_R(x))^{-1/2}\,dx. \tag{4.35}$$

Note that the above expressions are completely independent of ϵ. Thus, when evaluated at their corresponding single-well energies, we will abbreviate the phase shift derivatives as:

$$\phi_{12}^{'}(E_L) \equiv \frac{\partial}{\partial E}\phi_{12}(E_L(\epsilon),\epsilon), \tag{4.36}$$

$$\phi_{34}^{'}(E_R) \equiv \frac{\partial}{\partial E}\phi_{34}(E_R(\epsilon),\epsilon). \tag{4.37}$$

4.2.2 Expansion of quantization condition

We now wish to solve the double-well quantization condition (4.22) for the energy levels $E_I(\epsilon)$ and $E_{II}(\epsilon)$, or equivalently the energy shifts $\delta_L(\epsilon)$ and $\delta_R(\epsilon)$. Although this condition is a complicated nonlinear equation, it may be simplified by assuming that tunneling is weak and that detuning is small compared to the single-well level spacings.

Note that in the infinite barrier limit, there is no tunneling and each well can be quantized

using the single-well condition (3.21), which implies:

$$\phi_{12}(E_L(\epsilon), \epsilon) = \phi_{34}(E_R(\epsilon), \epsilon) = 0. \tag{4.38}$$

For a large barrier (weak tunneling), and small detuning, we expect the allowed energies $E(\epsilon)$ to be close to the single-well energies. We therefore expect the phase shifts to be close to zero. Consequently, we expect the cotangents in (4.22) to be close to $\cot(\pi/2)$. More precisely, if we assume

$$|\phi_{12}(E(\epsilon), \epsilon)| \ll \frac{\pi}{2}, \tag{4.39}$$

$$|\phi_{34}(E(\epsilon), \epsilon)| \ll \frac{\pi}{2}, \tag{4.40}$$

we can approximate the cotangents to first order:

$$\cot\left(\phi_{12}(E(\epsilon), \epsilon) + \frac{\pi}{2}\right) \approx -\phi_{12}(E(\epsilon), \epsilon), \tag{4.41}$$

$$\cot\left(\phi_{34}(E(\epsilon), \epsilon) + \frac{\pi}{2}\right) \approx -\phi_{34}(E(\epsilon), \epsilon), \tag{4.42}$$

Rewriting (4.22) now gives:

$$\phi_{12}(E(\epsilon), \epsilon) \cdot \phi_{34}(E(\epsilon), \epsilon) = \frac{1}{4}\exp(-2\theta_{23}(E(\epsilon), \epsilon)).) \tag{4.43}$$

At this point, it is convenient to substitute the double-well energies $E_I(\epsilon)$ and $E_{II}(\epsilon)$ into equation (4.43). We begin with the quantization condition for $E_{II}(\epsilon)$:

$$\phi_{12}(E_{II}(\epsilon), \epsilon) \cdot \phi_{34}(E_{II}(\epsilon), \epsilon) = \frac{1}{4}\exp(-2\theta_{23}(E_{II}(\epsilon), \epsilon)). \tag{4.44}$$

Writing E_{II} in terms of E_L and the energy shift δ_L gives:

$$\phi_{12}(E_L + \delta_L(\epsilon), \epsilon) \cdot \phi_{34}(E_L + \delta_L(\epsilon), \epsilon) \;=\; \frac{1}{4}\exp(-2\theta_{23}(E_L + \delta_L(\epsilon), \epsilon)). \tag{4.45}$$

Each side of the above equation can be further simplified by assuming $\delta_L(\epsilon)$ is small, or equivalently that the effect of tunneling on the shift in energy levels is weak.

The terms on the left hand side of (4.45) can be expanded when

$$\delta_L(\epsilon) \;\ll\; E_L(\epsilon), \tag{4.46}$$

which gives:

$$\begin{aligned}
&\phi_{12}(E_L(\epsilon) + \delta_L(\epsilon), \epsilon) \cdot \phi_{34}(E_L(\epsilon) + \delta_L(\epsilon), \epsilon) \\
&\approx \left[\phi_{12}(E_L(\epsilon), \epsilon) + \delta_L(\epsilon)\phi_{12}^{'}(E_L)\right] \cdot \left[\phi_{34}(E_L(\epsilon), \epsilon) + \delta_L(\epsilon)\phi_{34}^{'}(E_R)\right],
\end{aligned} \tag{4.47}$$

where note that the derivatives, as defined in (4.36) and (4.37), have no ϵ-dependence. Noting that $\phi_{12}(E_L(\epsilon), \epsilon) = 0$, and dropping second order and higher terms in $\delta_L(\epsilon)$ we obtain:

$$\phi_{12}(E_L(\epsilon) + \delta_L(\epsilon), \epsilon) \cdot \phi_{34}(E_L(\epsilon) + \delta_L(\epsilon), \epsilon) \;\approx\; \delta_L(\epsilon) \cdot \phi_{34}(E_L(\epsilon), \epsilon) \cdot \phi_{12}^{'}(E_L). \tag{4.48}$$

The right hand side of (4.45) can also be expanded for small $\delta_L(\epsilon)$, yielding:

$$\begin{aligned}
&\exp\left[-2\theta_{23}(E_L(\epsilon) + \delta_L(\epsilon), \epsilon)\right] \\
&\approx \exp\left[-2\theta_{23}(E_L(\epsilon), \epsilon)\right] \left[1 - 2\delta_L(\epsilon)\frac{\partial}{\partial E_L}\theta_{23}(E_L(\epsilon), \epsilon)\right].
\end{aligned} \tag{4.49}$$

Equating (4.48) and (4.49) gives the approximate quantization condition:

$$\begin{aligned}\delta_L(\epsilon)\cdot\phi_{34}(E_L(\epsilon),\epsilon)\cdot\phi_{12}^{'}(E_L) &= \frac{1}{4}\exp\left[-2\theta_{23}(E_L(\epsilon),\epsilon)\right] \\ &\quad\times\left[1-2\delta_L(\epsilon)\frac{\partial}{\partial E_L}\theta_{23}(E_L(\epsilon),\epsilon)\right], \end{aligned} \tag{4.50}$$

which can be solved for $\delta_L(\epsilon)$, giving:

$$\delta_L(\epsilon) = \frac{\exp\left[-2\theta_{23}(E_L(\epsilon),\epsilon)\right]}{4\phi_{12}^{'}(E_L)\cdot\phi_{34}(E_L(\epsilon),\epsilon)+2\exp\left[-2\theta_{23}(E_L(\epsilon),\epsilon)\right]\frac{\partial}{\partial E_L}\theta_{23}(E_L(\epsilon),\epsilon)}. \tag{4.51}$$

The analogous calculation for E_I gives:

$$\delta_R(\epsilon) = \frac{\exp\left[-2\theta_{23}(E_R(\epsilon),\epsilon)\right]}{4\phi_{34}^{'}(E_R)\cdot\phi_{12}(E_R(\epsilon),\epsilon)+2\exp\left[-2\theta_{23}(E_R(\epsilon),\epsilon)\right]\frac{\partial}{\partial E_R}\theta_{23}(E_R(\epsilon),\epsilon)}. \tag{4.52}$$

The exponential terms in the numerator and denominator of (4.51) and (4.52) decrease rapidly as the phase across the barrier $\theta_{23}(E(\epsilon),\epsilon)$ is increased. Thus, for weak tunneling (large barrier), the exponential term and its derivatives will be small. Thus the first term in the denominator of each equation will dominate, and we can neglect the second. Similarly, the numerator of each equation will be nearly constant for small changes in energy. Thus for weak tunneling, we can write:

$$\exp(-2\theta_{23}) \equiv \exp\left[-2\theta_{23}(E_L(\epsilon),\epsilon)\right]\approx\exp\left[-2\theta_{23}(E_R(\epsilon),\epsilon)\right] \tag{4.53}$$

$$\delta_L(\epsilon) = \frac{\exp(-2\theta_{23})}{4\phi_{12}^{'}(E_L)\cdot\phi_{34}(E_L(\epsilon),\epsilon)}, \tag{4.54}$$

$$\delta_R(\epsilon) = \frac{\exp(-2\theta_{23})}{4\phi_{34}^{'}(E_R)\cdot\phi_{12}(E_R(\epsilon),\epsilon)}. \tag{4.55}$$

Substituting these results into (4.21) gives an expression for the tunnel coupling as a function of detuning.

4.3 Analysis of detuning-dependence

Having derived an expression for the tunnel coupling t of a double-well, we now consider which types of potentials, if any, could allow t to depend on the detuning ϵ. We wil focus on the regime

$$t \ll \epsilon \ll \Delta_{L/R}. \tag{4.56}$$

In this regime, it is clear from Equation (4.21) that when $\delta_L(\epsilon) \propto 1/\epsilon$ and $\delta_R(\epsilon) \propto 1/\epsilon$, the factors of ϵ cancel, and t is independent of ϵ. However, if either $\delta_L(\epsilon)$ or $\delta_R(\epsilon)$ has a different ϵ-dependence, the resulting t may depend on ϵ. As we now show, $\delta_L(\epsilon)$ and $\delta_R(\epsilon)$ will have an aproximate $1/\epsilon$ dependence for typical potentials, resulting in an ϵ-independent tunnel coupling.

4.3.1 Typical case

It can be seen from equations (4.54) and (4.55) that all of the ϵ-dependence in $\delta_L(\epsilon)$ and $\delta_R(\epsilon)$ enters through the WKB phase shifts $\phi_{12}(E_R(\epsilon), \epsilon)$ and $\phi_{34}(E_L(\epsilon), \epsilon)$. Note that the phase shift of the left well is evaluated at the single-well energy of the right well and vice-versa. Let us suppose that the phase shift functions can be expanded about their corresponding single-well energies as follows:

$$\begin{aligned}
\phi_{12}(E_R(\epsilon), \epsilon) &= \phi_{12}(E_L(\epsilon) - \epsilon, \epsilon) && (4.57)\\
&\approx \phi_{12}(E_L(\epsilon), \epsilon) - \phi_{12}^{'}(E_L)\epsilon + \frac{1}{2}\phi_{12}^{''}(E_L)\epsilon^2 && (4.58)\\
&= -\phi_{12}^{'}(E_L)\epsilon + \frac{1}{2}\phi_{12}^{''}(E_L)\epsilon^2, && (4.59)\\
\phi_{34}(E_L(\epsilon), \epsilon) &= \phi_{34}(E_R(\epsilon) + \epsilon, \epsilon) && (4.60)\\
&\approx \phi_{34}(E_R(\epsilon), \epsilon) + \phi_{34}^{'}(E_R)\epsilon + \frac{1}{2}\phi_{34}^{''}(E_R)\epsilon^2 && (4.61)\\
&= \phi_{34}^{'}(E_R)\epsilon + \frac{1}{2}\phi_{34}^{''}(E_R)\epsilon^2. && (4.62)
\end{aligned}$$

The above equations show that the phase shifts are typically proportional to ϵ, plus higher order corrections. From equations (4.54) and (4.55), the corresponding energy shifts $\delta_L(\epsilon)$ and $\delta_R(\epsilon)$ will thus be approximately proportional to $1/\epsilon$, implying a nearly ϵ-independent tunnel coupling, with the possibility of small ϵ-dependent corrections. We discuss the results of numerical simulations used to look for these corrections in Chapter 5.

4.3.2 Exceptional case

Alternatively, let us consider if there is a case where the phase shifts cannot be expanded about their corresponding single-well energies. Such a situation arises if one of the derivatives of a phase shift is undefined. We will consider the first derivative in particular. An undefined first derivative occurs when a function has infinite slope. For a smooth potential, the phase shifts are continuous and increasing over the interval (E_0, ∞), where E_0 is the energy of the well's potential minimum. Such a function can only have infinite slope at one point, E_0. For such a potential, E_0 cannot occur near the single-well energy, since these energies correspond to different phases, 0 and $\pi/2$ respectively. However, if the potential has a discontinuous first derivative, the corresponding phase shift can have infinite slope at energies other than E_0.

One way to construct such a potential is to create a piecewise "well-within-a-well." For instance, see Figure 4.2. For energies below the transition energy E_T, the WKB phase will be determined solely by the potential in region II. For energies above E_T, the phase will be determined by the potential in all of the regions. The sum of the phases in regions I and III is equal to the phase across a smooth single-well with a minimum at E_T. Thus, if one side of a double-well is constructed in this fashion, with E_T near the single-well energy, the corresponding phase shift cannot be approximated by a Taylor series, making a range of ϵ-dependence possible for the tunnel coupling. Note that we have actually already assumed that the phase shifts can be expanded about the single-well energies in Equation (4.47),

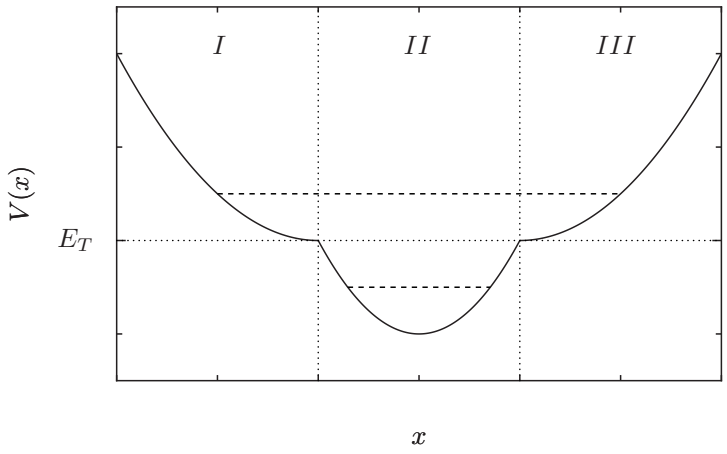

Figure 4.2: Example of a well having a discontinuous first derivative of the WKB phase integral. The phase across regions I and III is exactly that of a smooth well with a minimum at E_T. Region II, with a different phase integral, has been spliced in the middle, creating a discontinuous derivative of the phase integral at E_T. Two example energy levels are shown, the lowest having phase due to only Region II, and the highest having phase contributed by all regions. In principle, any shape of potential could be used, as long as there is a critical point at E_T.

so we cannot consistently place the single-well energy exactly at the point of discontinuous derivative, without altering our analysis. However, if we place it close, the above analysis suggests that we may see a non-trivial ϵ-dependence.

At first, potentials of the type shown in Figure 4.2 may seem artificial. However, such a potential can be seen as a simplified model of a localized impurity. Such impurities do occur in semiconductor quantum dots, motivating our further study of these potentials.

4.3.3 Detuning-dependence of a modified square double-well

We now consider a double square well constructed by the procedure described above. Consider the potential shown in Figure 4.3. We define V_D and a as the respective depth and width of both "inner" square wells and a as the width of both the "outer" wells. We also

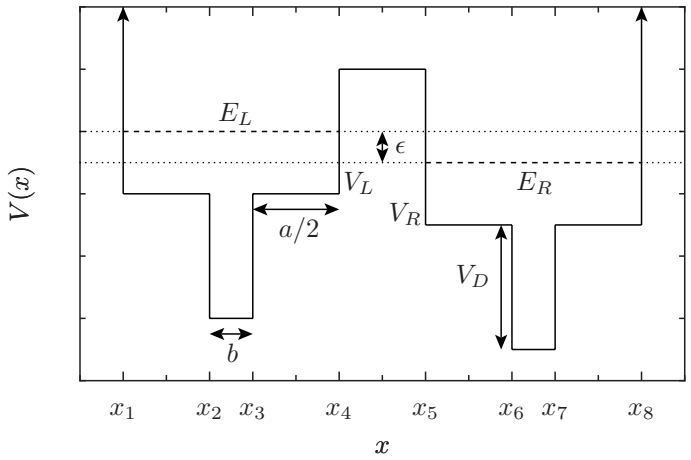

Figure 4.3: A modified square double-well potential. Each well consists of a square well of width $a + b$ containing another well of width b in its center. The potential is valued V_L and V_R at the left and right outer wells respectively. The inner well potential is lower by V_D than that of the corresponding outer well. The single-well energies E_L and E_R are drawn as dashed lines.

define $V_L(\epsilon)$ and $V_R(\epsilon)$ as the potential of the outer wells, giving the useful relations:

$$\Delta_L = E_L(\epsilon) - V_L(\epsilon) - V_D, \tag{4.63}$$

$$\Delta_R = E_R(\epsilon) - V_R(\epsilon) - V_D. \tag{4.64}$$

When $E_L(\epsilon) > V_R(\epsilon)$ and $E_R(\epsilon) > V_L(\epsilon)$, the phase integrals $\phi_{12}(E_R(\epsilon), \epsilon)$ and $\phi_{34}(E_L(\epsilon), \epsilon)$ are:

$$\begin{aligned}
\phi_{12}(E_R(\epsilon), \epsilon) &= \frac{\sqrt{2m}}{\hbar} \int_{x_1}^{x_2} \sqrt{E_R(\epsilon) - V_L(\epsilon)}\, dx \\
&\quad + \frac{\sqrt{2m}}{\hbar} \int_{x_2}^{x_3} \sqrt{E_R(\epsilon) - V_L(\epsilon) - V_D}\, dx \\
&\quad + \frac{\sqrt{2m}}{\hbar} \int_{x_3}^{x_4} \sqrt{E_R(\epsilon) - V_L(\epsilon)}\, dx - \frac{\pi}{2}, \qquad (4.65) \\
\phi_{34}(E_L(\epsilon), \epsilon) &= \frac{\sqrt{2m}}{\hbar} \int_{x_5}^{x_6} \sqrt{E_L(\epsilon) - V_R(\epsilon)}\, dx \\
&\quad + \frac{\sqrt{2m}}{\hbar} \int_{x_6}^{x_7} \sqrt{E_L(\epsilon) - V_R(\epsilon) - V_D}\, dx \\
&\quad + \frac{\sqrt{2m}}{\hbar} \int_{x_7}^{x_8} \sqrt{E_L(\epsilon) - V_R(\epsilon)}\, dx - \frac{\pi}{2}. \qquad (4.66)
\end{aligned}$$

Integrating the above and simplifying gives:

$$\begin{aligned}
\phi_{12}(E_R(\epsilon), \epsilon) &= \frac{\sqrt{2m}}{\hbar} \left[a\sqrt{E_R(\epsilon) - V_L(\epsilon)} + b\sqrt{E_R(\epsilon) - V_L(\epsilon) - V_D} \right] - \frac{\pi}{2} \qquad (4.67) \\
&= \frac{\sqrt{2m}}{\hbar} \left[a\sqrt{E_L(\epsilon) - V_L(\epsilon) - \epsilon} \right. \\
&\quad \left. + b\sqrt{E_L(\epsilon) - V_L(\epsilon) - V_D - \epsilon} \right] - \frac{\pi}{2}, \qquad (4.68) \\
\phi_{12}(E_R(\epsilon), \epsilon) &= \frac{\sqrt{2m}}{\hbar} \left[a\sqrt{E_L(\epsilon) - V_R(\epsilon)} + b\sqrt{E_L(\epsilon) - V_R(\epsilon) - V_D} \right] - \frac{\pi}{2} \qquad (4.69) \\
&= \frac{\sqrt{2m}}{\hbar} \left[a\sqrt{E_R(\epsilon) - V_R(\epsilon) + \epsilon} \right. \\
&\quad \left. + b\sqrt{E_R(\epsilon) - V_R(\epsilon) - V_D + \epsilon} \right] - \frac{\pi}{2}. \qquad (4.70)
\end{aligned}$$

Further simplification using (4.63) and (4.64) yields our final form for these expressions:

$$\begin{aligned}
\phi_{12}(E_R(\epsilon), \epsilon) &= \frac{\sqrt{2m}}{\hbar} \left[a\sqrt{(\Delta_L - V_D) - \epsilon} + b\sqrt{\Delta_L - \epsilon} \right] - \frac{\pi}{2}, \qquad (4.71) \\
\phi_{34}(E_L(\epsilon), \epsilon) &= \frac{\sqrt{2m}}{\hbar} \left[a\sqrt{(\Delta_R - V_D) + \epsilon} + b\sqrt{\Delta_R + \epsilon} \right] - \frac{\pi}{2}, \qquad (4.72)
\end{aligned}$$

for $(\Delta_L - V_D) > \epsilon$.

With an explicit form for these phase shifts, the ϵ-dependence is easy to determine. For positive $\epsilon \ll (\Delta_L - V_D)$ and $\epsilon \ll (\Delta_R - V_D)$, both of the radicals in each equation can be approximated to first order in ϵ, leaving the trivial linear ϵ dependence, plus higher-order terms. On the other hand, if V_D is chosen close to Δ_L and/or Δ_R, there may be a regime where:

$$(\Delta_L - V_D) \ll \epsilon \ll \Delta_L, \tag{4.73}$$

$$(\Delta_R - V_D) \ll \epsilon \ll \Delta_R. \tag{4.74}$$

In this regime, the outer left well will be high enough that it becomes clasically forbidden, so the first term of (4.71) disappears, leaving the linear ϵ-dependence of the second term. On the other hand, the first term of (4.72) remains, and is dominated by ϵ, giving a non-trivial $\sqrt{\epsilon}$ dependence, plus higher order terms. Note that the $\sqrt{\epsilon}$ dependence is unique to the square well, although other potentials yield alternative non-trivial behavior. We focus on the square well because for small ϵ, $\sqrt{\epsilon}$ dominates over the linear term from the expansion of the second radical in (4.72).

In terms of the tunnel coupling, the above WKB analysis predicts that potentials of the shape shown in Figure 4.3 can result in a t that varies with ϵ. WKB suggests a transition at $\epsilon \approx \Delta_{L/R}$. For $\epsilon \ll \Delta_{L/R}$, we find the tunnel coupling and splitting will have the trivial constant and $1/\epsilon$ dependence respectively. For $\epsilon \gg \Delta_{L/R}$, WKB suggests a $\delta_R(\epsilon)$ with $\epsilon^{-1/2}$ dependence and therefore a tunnel coupling with an $\epsilon^{1/4}$ dependence. However, note that the validity of WKB in the regime described above is questionable. WKB is valid when the phase integrals are much greater than 1. Not only are the phase integrals in this case of order 1, in the "outer well" regions, they are much less than 1. In Chapter 6, we give the results of numerical calculations used to test the predictions described above.

In conclusion, we have shown that WKB predicts two possible sources for ϵ-dependence of t. First, we found that typical potentials should have, as commonly-expected, ϵ-independent tunnel couplings to first order, but with possible ϵ-dependent corrections. We also described a particular class of potentials that allow for non-trivial ϵ-dependence, and derived a $\epsilon^{1/4}$ dependence for the tunnel coupling of a modified square well. We test these predictions numerically in Chapter 6 and Chapter 7 respectively.

Chapter 5

Numerical Methods

The reduced double-well Hamiltonian of Chapter 2 and the WKB solutions of Chapter 4 provide convenient, simple formulas for the tunnel coupling of a double-well. However, this convenience comes at the cost of accuracy. It is therefore necessary to test the theoretical predictions of the previous chapters by comparing them to the exact solutions of particular potentials. No exact analytic solutions are available for general detuned double-wells, so we must rely on numerical methods.

By using numerical methods to solve the time-independent Schrödinger equation, we can determine the eigenstates and energy levels of a potential to any desired precision. For a particle of mass m bound in a 1-dimensional potential $V(x)$, the Schrödinger equation is a linear, second-order, ordinary differential equation:

$$\left[-\frac{\hbar^2}{2m}\frac{d^2}{dx^2} + V(x)\right]\psi(x) \;=\; E\psi(x), \tag{5.1}$$

where allowed values of E have square-integrable solutions, consistent with the normalization

condition:

$$\int_{-\infty}^{\infty} \psi^*(x)\psi(x)\,dx \;=\; 1. \tag{5.2}$$

We now present two methods for solving (5.1) numerically: the finite difference method (Section 5.1), and the transfer matrix method (Section 5.2).

5.1 Finite difference method

The finite difference method is a standard technique for finding the approximate numerical solutions of a differential equation. In this section, we present the basic procedure and discuss the issue of convergence.

5.1.1 Motivation and derivation

We now motivate and derive the finite difference method, following [1]. The fundamental idea behind the finite difference method is to divide a real interval into subintervals, and approximate a function on that interval by its set of values at the center of each subinterval. Let (x_{min}, x_{max}) be a real interval. Dividing this interval into N equally-spaced subintervals and defining x_n as the midpoint of the nth one gives:

$$x_n \;=\; x_{min} + h\left(n - \frac{1}{2}\right) \quad \text{for } n \in \{1, 2, \ldots, N\}, \tag{5.3}$$

$$h \;=\; \frac{x_{max} - x_{min}}{N}, \tag{5.4}$$

where h is the *grid spacing* of the discrete points. A function $\psi(x)$ defined on the full interval can be approximated by its value at each point x_n:

$$\psi_n \;\equiv\; \psi(x_n). \tag{5.5}$$

We can also define operators which act on discrete functions of x_n. The *forward difference* Δ_h, *backward difference* ∇_h, and *central difference* δ_h are defined as:

$$\Delta_h \psi_n = \psi_{n+1} - \psi_n, \tag{5.6}$$

$$\nabla_h \psi_n = \psi_n - \psi_{n-1}, \tag{5.7}$$

$$\delta_h \psi_n = \psi_{n+1/2} - \psi_{n-1/2}. \tag{5.8}$$

These *finite difference* operators are somewhat analogous to derivatives, and indeed they can be used to approximate derivatives under the appropriate conditions.

The Taylor expansion of $\psi(x)$ provides the necessary connnection between the derivative $d\psi/dx$ and the finite difference $\Delta_h \psi_n / \Delta_h x_n$. If $\psi(x)$ is infinitely differentiable, we may write:

$$\psi_{n+1} = \psi(x_n + \Delta_h x_n) = \psi_n + \psi'_n \Delta_h x_n + \frac{1}{2}\psi''_n (\Delta_h x_n)^2 + \mathcal{O}((\Delta_h x_n)^3), \tag{5.9}$$

$$\psi_{n-1} = \psi(x_n - \Delta_h x_n) = \psi_n - \psi'_n \Delta_h x_n + \frac{1}{2}\psi''_n (\Delta_h x_n)^2 + \mathcal{O}((\Delta_h x_n)^3). \tag{5.10}$$

Equation (5.9) may be rearranged to give:

$$\psi'_n = \frac{\psi(x_n + \Delta_h x_n) - \psi(x_n)}{\Delta_h x_n} + \mathcal{O}(\Delta_h x_n) \tag{5.11}$$

$$= \frac{\Delta_h}{\Delta_h x_n}\psi_n + \mathcal{O}(h). \tag{5.12}$$

In other words, the first difference of ψ_n divided by the grid spacing is approximately equal to the the first derivative of $\psi(x_n)$. The difference between the two, known as the *truncation error*, decreases with the grid spacing h, as one might expect.

We can also derive a similar equation for the second derivative. Adding (5.9) to (5.10)

yields the equation:

$$\psi(x_n + \Delta_h x_n) + \psi(x_n - \Delta_h x_n) \;=\; 2\psi(x_n) + \psi_n''(\Delta_h x_n)^2 + \mathcal{O}((\Delta_h x_n)^3), \tag{5.13}$$

Solving for the second derivative, we find:

$$\psi_n'' \;=\; \frac{\psi(x_n + \Delta_h x_n) + \psi(x_n - \Delta_h x_n) - 2\psi(x_n)}{(\Delta_h x_n)^2} + \mathcal{O}(\Delta_h x_n) \tag{5.14}$$

$$\;=\; \frac{\psi_{n+1} + \psi_{n-1} - 2\psi_n}{(\Delta_h x_n)^2} + \mathcal{O}(h) \tag{5.15}$$

$$\;=\; \frac{\delta_h^2}{(\Delta_h x_n)^2}\psi_n + \mathcal{O}(h). \tag{5.16}$$

The second derivative of $\psi(x)$ can thus be approximated by the second central difference of ψ_n divided by h^2, with a truncation error on the order of h.

5.1.2 Application to the Schrödinger equation

We may now write a finite difference equation approximating the time-independent Schrödinger equation (5.1):

$$\left[-\frac{\hbar^2}{2m}\frac{\delta_h^2}{h^2} + V(x_n)\right]\psi_n \;=\; E\psi_n. \tag{5.17}$$

Note that the term in brackets is a linear operator, which we shall refer to as the discrete Hamiltonian H_h. Also note that ψ_n can be thought of as a vector of length n. We therefore have a linear system of equations which can be represented by a matrix. Consequently this representation of the system can be easily manipulated in software.

We have stated the problem in the x_n basis, which was used for the finite difference simulations described in later chapters. However, any basis could be used for the representation of H_h. For instance, H_h could be written in the basis of infinite square well solutions, which has

the advantage of automatically projecting out solutions inconsistent with the normalization condition (5.2).

Note that Equation (5.17) has the form of an eigenvalue equation:

$$H_h\psi_n \;=\; E\psi_n. \tag{5.18}$$

Furthermore, although the matrix representation of H_h may be very large, $V(x_n)$ is diagonal and δ_h is tridiagonal, so H_h is sparse. The eigenvalue problem can thus be solved relatively quickly using standard software packages. In particular, the MATLAB `eigs()` routine was used for the simulations in this thesis.

The MATLAB `eigs()` routine uses the Lanczos algorithm for finding the eigenvalues and eigenvectors of a sparse matrix. The details of this algorithm can be found in [8]. The main principle behind the Lanczos method is the generation of the powers of a matrix, known as the Krylov sequence. For a Hermitian matrix A and a random vector $|\psi\rangle$:

$$A^n|\psi\rangle \;\rightarrow\; \lambda^n\langle\lambda|\psi\rangle|\lambda\rangle \;\text{ as } n\rightarrow\infty, \tag{5.19}$$

where λ is the largest eigenvalue of A and $|\lambda\rangle$ is the corresponding eigenvector. One can thus approximate λ and $|\lambda\rangle$ by repeatedly applying A to a random vector. The second largest eigenvalue can be found by applying the projector $I-|\lambda\rangle\langle\lambda|$ to A, and repeating the procedure, and so on for subsequent eigenvalues. Similarly, the smallest eigenvalues can be found by applying the procedure to $\lambda - A$, where λ is the largest eigenvalue of A.

5.1.3 Errors and convergence

The above derivation gives a truncation error on the order of the grid spacing h. As the grid is made denser, the exact solution of the difference equation will converge to that of the

differential equation. However, our derivation depended on the assumption that the solution $\psi(x)$ was infinitely differentiable. Equation (5.1) implies that if the nth derivative of $V(x)$ is undefined at some point, then the $(n+2)$nd derivative of $\psi(x)$ will also be undefined. In this case, the equations (5.9) and (5.10) are invalid. However, if the all derivatives of $\psi(x)$ lower than nth order exist, we can write $\psi(x)$ as an nth order partial Taylor expansion plus an integral remainder term. If $V(x)$ is differentiable the third derivative of $\psi(x)$ will also exist, allowing a partial Taylor expansion up to second order. Thus, as long as $V(x)$ is continuous, we can still approximate the Schrödinger equation by Equation (5.17). However, the truncation error is no longer of order h and convergence is not guaranteed as h becomes small.

Also note that the truncation error is not the only error associated with the method we have described. By using the Lanzcos algorithm, we only solve the difference equation to a finite precision, introducing *round-off error*. In general (c.f. [1]), the round-off error tends to increase as the grid spacing decreases. Thus, the number of Lanczos iterations must be increased as the grid size is decreased.

The above considerations suggest that truncation and round-off error can be neglected for differentiable potentials as long as enough Lanczos iterations are used. However, for non-differentiable functions, such as the modified square potential discussed in Section 4.3.2, another method is necessary.

5.2 Transfer matrix method

Piecewise constant potentials, although not differentiable, lend themselves to precise numerical solution through the manipulation of 2×2 matrices. We now describe this method, known as the transfer matrix method, following [12] and [14].

5.2.1 Transfer matrices

We define a piecewise potential $V(x)$ with N boundaries between regions of constant potential. For now, we will assume that the rightmost and leftmost regions extend to $\pm\infty$, i.e. that there are no infinite potential walls. Let $a_n, n \in \{1, \ldots, N\}$, be the coordinates of the nth boundary. Let $V_n, n \in \{1, \ldots, N+1\}$, be the constant potential value to the left of the nth boundary. If $\psi_n(x)$ is the wavefunction to the left of the nth boundary, the following matching conditions must be satisfied:

$$\psi_n(a_n) = \psi_{n+1}(a_n), \tag{5.20}$$

$$\psi'_n(a_n) = \psi'_{n+1}(a_n). \tag{5.21}$$

We thus need to find the wavefunctions and their derivatives for each region.

Within each region of constant potential, the 1-dimensional, time-independent Schrödinger equation is:

$$\left[-\frac{\hbar^2}{2m}\frac{d^2}{dx^2} + V\right]\psi(x) = E\psi(x), \tag{5.22}$$

where V is constant, and as usual, $\psi(x)$ and E are the eigenstate wave function and corresponding energy. This equation can have one of three types of solutions depending on the value of E:

$$\psi(x) = \begin{cases} Ae^{-\kappa x} + Be^{\kappa x} & (E < V), \\ Ae^{ikx} + Be^{-ikx} & (E > V), \\ A + Bx & (E = V), \end{cases} \tag{5.23}$$

where A and B are determined by the boundary conditions and k and κ are:

$$k = \frac{1}{\hbar}\sqrt{2m(E-V)}, \tag{5.24}$$

$$\kappa = \frac{1}{\hbar}\sqrt{2m(V-E)}. \tag{5.25}$$

The derivatives of (5.23) are:

$$\psi'(x) = \begin{cases} -\kappa A e^{-\kappa x} + \kappa B e^{\kappa x} & (E < V), \\ ikAe^{ikx} - ikBe^{-ikx} & (E > V), \\ B & (E = V). \end{cases} \tag{5.26}$$

The wavefunctions (5.23) and derivatives (5.26) may be written in matrix form. For $E < V$, we write:

$$\begin{bmatrix} \psi(x) \\ \psi'(x) \end{bmatrix} = \begin{bmatrix} e^{-\kappa x} & e^{\kappa x} \\ -\kappa e^{-\kappa x} & \kappa e^{\kappa x} \end{bmatrix} \begin{bmatrix} A \\ B \end{bmatrix} \tag{5.27}$$

$$= \begin{bmatrix} 1 & 1 \\ -\kappa & \kappa \end{bmatrix} \begin{bmatrix} e^{-\kappa x} & 0 \\ 0 & e^{\kappa x} \end{bmatrix} \begin{bmatrix} A \\ B \end{bmatrix}, \tag{5.28}$$

for $E > V$:

$$\begin{bmatrix} \psi(x) \\ \psi'(x) \end{bmatrix} = \begin{bmatrix} e^{ikx} & e^{-ikx} \\ ike^{ikx} & -ike^{-ikx} \end{bmatrix} \begin{bmatrix} A \\ B \end{bmatrix} \tag{5.29}$$

$$= \begin{bmatrix} 1 & 1 \\ ik & -ik \end{bmatrix} \begin{bmatrix} e^{ikx} & 0 \\ 0 & e^{-ikx} \end{bmatrix} \begin{bmatrix} A \\ B \end{bmatrix}, \tag{5.30}$$

and for $E = V$:

$$\begin{bmatrix} \psi(x) \\ \psi'(x) \end{bmatrix} = \begin{bmatrix} 1 & x \\ 0 & 1 \end{bmatrix} \begin{bmatrix} A \\ B \end{bmatrix} \tag{5.31}$$

$$= \begin{bmatrix} 1 & 0 \\ 0 & 1 \end{bmatrix} \begin{bmatrix} 1 & x \\ 0 & 1 \end{bmatrix} \begin{bmatrix} A \\ B \end{bmatrix}. \tag{5.32}$$

The matrix representation of $\psi(x)$ and $\psi'(x)$ in each of the cases (5.28), (5.30), and (5.32) takes the general form:

$$\begin{bmatrix} \psi(x) \\ \psi'(x) \end{bmatrix} = K(V)E(V,x) \begin{bmatrix} A \\ B \end{bmatrix}. \tag{5.33}$$

We can now write the matching conditions (5.20) and (5.21) as matrix equations in terms of $K(V)$ and $E(V,x)$:

$$\begin{bmatrix} \psi_n(a_n) \\ \psi'_n(a_n) \end{bmatrix} = \begin{bmatrix} \psi_{n+1}(a_n) \\ \psi'_{n+1}(a_n) \end{bmatrix}, \tag{5.34}$$

$$K(V_n)E(V_n,a_n) \begin{bmatrix} A_n \\ B_n \end{bmatrix} = K(V_{n+1})E(V_{n+1},a_n) \begin{bmatrix} A_{n+1} \\ B_{n+1} \end{bmatrix}, \tag{5.35}$$

where we have labeled the potential in region n as V_n. Left-multiplying both sides by $E^{-1}(V_n,a_n)K^{-1}(V_n)$ yields an equation relating the coefficients for region n to those for

region $n+1$:

$$\begin{bmatrix} A_n \\ B_n \end{bmatrix} = E^{-1}(V_n, a_n)K^{-1}(V_n)K(V_{n+1})E(V_{n+1}, a_n) \begin{bmatrix} A_{n+1} \\ B_{n+1} \end{bmatrix} \tag{5.36}$$

$$\equiv T_n \begin{bmatrix} A_{n+1} \\ B_{n+1} \end{bmatrix}. \tag{5.37}$$

The operator T_n is known as a *transfer matrix*.

5.2.2 Bound states

By applying multiple transfer matrices, the wavefunction coefficients in region 1, can be related to those in region $N+1$, which can be used to determine the bound state energy levels. We define the operator $\mathcal{T}$ to be:

$$\mathcal{T} = T_1 T_2 \dots T_N, \tag{5.38}$$

allowing us to write:

$$\begin{bmatrix} A_1 \\ A_2 \end{bmatrix} = \mathcal{T} \begin{bmatrix} A_{N+1} \\ B_{N+1} \end{bmatrix}. \tag{5.39}$$

Bound states must not blow up as $x \to \pm\infty$, which implies:

$$A_1 = B_{N+1} = 0. \tag{5.40}$$

Combining (5.39) and (5.40) gives a constraint on the elements of $\mathcal{T}$ for bound states:

$$\begin{aligned} A_1 &= t_{11}A_{N+1} + t_{12}B_{N+1}, && (5.41)\\ 0 &= t_{11}A_{N+1}, && (5.42)\\ t_{11} &= 0, && (5.43) \end{aligned}$$

where t_{ij} are the elements of $\mathcal{T}$. For any value of E, the matrix $\mathcal{T}$ can be easily constructed numerically, and standard zero-finding algorithms can be applied to find the zeros of t_{11}, and thus the bound state energies, to any desired precision. Note that we have assumed the potential to be finite everywhere. However, we can derive a similar condition for the bound states of a piecewise constant potential with infinite barriers on either side.

For the infinite barrier case, we rewrite the transfer matrix $\mathcal{T}$ as:

$$\mathcal{T} = E^{-1}(V_1, a_1)K^{-1}(V_1)\mathcal{M}K(V_{N+1})E(V_{N+1}, a_N), \quad (5.44)$$

where $\mathcal{M}$ depends only on the potentials $\{V_2, \ldots, V_N\}$ and not V_1 or V_{N+1}. In a classically forbidden region, the inverses of $E(V, x)$ and $K(V)$ are:

$$\begin{aligned} E^{-1}(V, x) &= \begin{bmatrix} e^{-\kappa x} & 0 \\ 0 & e^{\kappa x} \end{bmatrix}, && (5.45)\\ K^{-1}(V) &= \frac{1}{2}\begin{bmatrix} 1 & -\frac{1}{\kappa} \\ 1 & \frac{1}{\kappa} \end{bmatrix}. && (5.46) \end{aligned}$$

The transfer matrix $\mathcal{T}$ then becomes:

$$\mathcal{T} = \frac{1}{2\kappa_1}\begin{bmatrix} \kappa_1 e^{\kappa_1 a_1} & -e^{\kappa_1 a_1} \\ \kappa_1 e^{-\kappa_1 a_1} & e^{\kappa_1 a_1} \end{bmatrix}\mathcal{M}\begin{bmatrix} e^{-\kappa_{N+1} a_N} & e^{\kappa_{N+1} a_N} \\ -\kappa_{N+1} e^{-\kappa_{N+1} a_N} & \kappa_{N+1} e^{\kappa_{N+1} a_N} \end{bmatrix}. \quad (5.47)$$

Writing the elements of $\mathcal{M}$ as m_{ij} and multiplying gives:

$$\begin{aligned}\mathcal{T} &= \frac{1}{2\kappa_1}\begin{bmatrix} \kappa_1 e^{\kappa_1 a_1} m_{11} - e^{k_1 a_1} m_{21} & \kappa_1 e^{\kappa_1 a_1} m_{12} - e^{\kappa_1 a_1} m_{22} \\ \kappa_1 e^{-\kappa_1 a_1} m_{11} + e^{k_1 a_1} m_{21} & \kappa_1 e^{-\kappa_1 a_1} m_{12} + e^{\kappa_1 a_1} m_{22} \end{bmatrix} \\ &\times \begin{bmatrix} e^{-\kappa_{N+1} a_N} & e^{\kappa_{N+1} a_N} \\ -\kappa_{N+1} e^{-\kappa_{N+1} a_N} & \kappa_{N+1} e^{\kappa_{N+1} a_N} \end{bmatrix}. \end{aligned} \tag{5.48}$$

To write the quantization condition (5.43), we only need to calculate t_{11}:

$$\begin{aligned} t_{11} &= \frac{1}{2\kappa_1}\left[(\kappa_1 e^{\kappa_1 a_1} m_{11} - e^{\kappa_1 a_1} m_{21})(e^{-\kappa_{N+1} a_N}) \right. \\ &\quad \left. + (\kappa_1 e^{\kappa_1 a_1} m_{12} - e^{\kappa_1 a_1} m_{22})(-\kappa_{N+1} e^{-\kappa_{N+1} a_N})\right] \qquad (5.49) \\ &= \frac{1}{2} e^{\kappa_1 a_1 - \kappa_{N+1} a_N}(m_{11} - \frac{m_{21}}{\kappa_1} - \kappa_{N+1} m_{12} + \frac{\kappa_{N+1} m_{22}}{\kappa_1}). \qquad (5.50) \end{aligned}$$

Letting $\kappa \equiv \kappa_1 = \kappa_{N+1} \to \infty$, the quantization condition becomes:

$$m_{11} - \kappa m_{12} + m_{22} = 0. \tag{5.51}$$

Energies satisfying the above constraint correspond to valid, normalizable bound states. Since $\kappa \to \infty$, we can write the infinite barrier quantization condition simply as:

$$m_{12} = 0. \tag{5.52}$$

As with the finite-barrier case, this condition can be solved to any desired precision using standard zero-finding algorithms.

In summary, the finite difference method and the transfer matrix method provide accurate numerical solutions for a wide range of potentials. Differentiable potentials can be solved by the finite difference method, although convergence is not guaranteed unless the potential

is infinitely differentiable. Alternatively, piecewise constant potentials with finite or infinite barriers on the edges can be solved to any desired precision by the transfer matrix method.

Chapter 6

Leading Order Behavior

In Section 4.3, we saw that to leading order, WKB predicts a detuning-independent tunnel coupling for typical potentials, but allows detuning-dependence for certain exceptional potentials. In particular, we examined a modified square well for which WKB predicts an $\epsilon^{-1/2}$ dependence for the energy shift δ_L, and therefore an $\epsilon^{1/4}$ dependence for t. This chapter describes the numerical simulations used to test these predictions. The typical case is tested using a piecewise parabolic potential in Section 6.1, followed by the modified square double-well in Section 6.2.

6.1 Parabolic double-well

A piecewise parabolic potential was used to test the predictions made for typical double-wells in Section 4.3.1. This potential is composed of four regions: the left and right wells, and the left and right halves of the barrier. The left and right wells have the same curvature, but are offset by the detuning. Parameters were chosen to ensure the potential and its derivative are continuous everywhere. For a double-well with a barrier of height V_b, minimum-to-minimum width w, detuning ϵ, and left/right well characteristic frequency ω, the explicit form of the

potential is:

$$V_\epsilon(x) = \begin{cases} \frac{m\omega^2}{2}\left(x + w/2\right)^2 + \frac{\epsilon}{2} & \text{if } x < x_L, \\ -\frac{m\omega_L^2}{2}x^2 + V_b & \text{if } x_L \le x < 0, \\ -\frac{m\omega_R^2}{2}x^2 + V_b & \text{if } 0 \le x < x_R, \\ \frac{m\omega^2}{2}\left(x - w/2\right)^2 - \frac{\epsilon}{2} & \text{if } x < x_R, \end{cases} \tag{6.1}$$

where x_L, x_R, ω_L, and ω_R are given by:

$$x_L = \frac{4}{wm\omega^2}\left(V_b - \frac{\epsilon}{2}\right) - \frac{w}{2}, \tag{6.2}$$

$$x_R = \frac{w}{2} - \frac{4}{wm\omega^2}\left(V_b + \frac{\epsilon}{2}\right), \tag{6.3}$$

$$\omega_L = \omega\sqrt{\frac{w}{-2x_L} - 1}, \tag{6.4}$$

$$\omega_R = \omega\sqrt{1 - \frac{w}{2x_R}}. \tag{6.5}$$

Specific parameters were chosen to ensure that $t \ll \epsilon \ll \hbar\omega$, and to give a ratio $t/\hbar\omega$ comparable to those seen in actual devices (cf. [16]). These parameters are given in Table 6.1. For a range of detunings, the tunnel splitting δ was determined using both the finite difference method (Section 5.1) and the numerical solution of the full WKB quantization condition (3.55). Using Equation (2.63), the tunnel coupling at zero detuning, t_0, was calculated for each method, and appears in Table 6.1. For each value of the detuning, the value $\delta - \epsilon$ is plotted in Figure 6.1.

6.1.1 Discussion

The quantity $\delta - \epsilon$, plotted in Figure 6.1, is connected to the tunnel coupling through Equation (2.64). An epsilon dependence of ϵ^{-1} (slope -1 on a log-log plot) for the above quantity

Parameter		Value	Units
Min-to-min width	w	5.5	$[\sqrt{\hbar/m\omega}]$
Barrier height	V_b	3.5	$[\hbar\omega]$
Detuning	ϵ	0.001–0.1	$[\hbar\omega]$
Tunnel coupling (exact, $\epsilon = 0$)	$t_0^{(exact)}$	0.0017	$[\hbar\omega]$
Tunnel coupling (WKB, $\epsilon = 0$)	$t_0^{(WKB)}$	0.0015	$[\hbar\omega]$

Table 6.1: Parameters of the piecewise, parabolic double-well potential. The width w represents the spacing between the minima of the two wells. The two tunnel couplings given were determined using the numerical solution of the WKB quantization condition and the finite difference method.

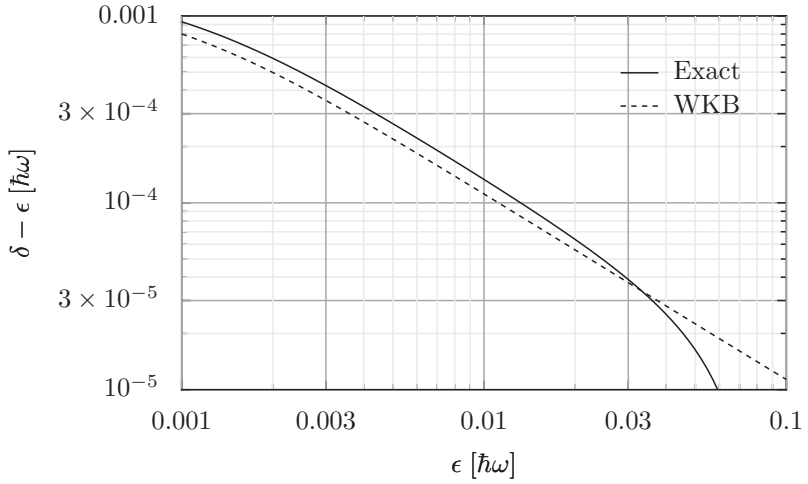

Figure 6.1: Numerical results for the piecewise, parabolic double-well potential. The detuning on the horizontal axis ranges from $\epsilon \sim t$ to $\epsilon \sim \hbar\omega$. The exact and WKB solutions show similar ϵ-dependence when $\epsilon \ll \hbar\omega$, consistent with an ϵ-independent tunnel coupling for $t \ll \epsilon \ll \hbar\omega$.

corresponds to an ϵ-independent tunnel coupling. Note that the value of the splitting predicted by WKB differs from that of the exact solution, but the ϵ-dependence of the two agree until the detuning becomes large. For detunings in the middle of the range, both WKB and the exact solution show a detuning-dependence very near to ϵ^{-1}. Variations in the ϵ-dependence at other detunings do not necessarily imply a different ϵ-dependence for the tunnel coupling. For smaller detunings, Equation (2.64) is not valid, and the relationship between t and δ becomes more complicated. For large detunings, the condition (2.69)

is not met, and the two-state, reduced Hamiltonian becomes invalid. The results shown in Figure 6.1 are thus consistent with the WKB prediction that the leading-order behavior of the tunnel coupling should be ϵ-independent.

6.2 Modified square double-well

According to WKB analysis, the modified square double-well of Section 4.3.2 (Figure 4.3) allows for a tunnel coupling with an ϵ-dependent leading order term. This prediction was checked numerically, using both the numerical solution of the WKB quantization condition (3.55) and the transfer matrix method of Section 5.2.

Unlike single parabolic wells, WKB does not predict the exact energy levels for single square wells. The non-trivial behavior described in Section 4.3.2 requires the single-well states to be very close to the bottom of the outer well, which is impossible to achieve simultaneously for the WKB and exact single well energy levels. In order to place the single-well energies at the same level for both the WKB and exact numerical solutions, different depths were chosen for the inner wells for each method. The relationship between the depth and width of the inner well was chosen so as to place the single well energy at a value of $0.002E_0$ above the bottom of the outer well, where E_0 is the exact ground state energy of the outer well in the absence of the inner well. All other parameters were as in the previous section, and are given in Table 6.2. The numerical results are shown in Figure 6.2

6.2.1 Discussion

Figure 6.2 shows interesting behavior for the exact solution of the WKB quantization condition (dashed line). For small detuning, the familiar ϵ^{-1} dependence of the energy shift is evident from its slope. However, for larger detunings, there is a sharp transition to a $\epsilon^{-1/2}$ dependence. This is exactly the transition predicted in Section 4.3.3, and occurs at $\epsilon \sim 0.002$,

Parameter		Value	Units
Exact single well energy	E_0	1	$[E_0]$
WKB single well energy	E_{WKB}	1/4	$[E_0]$
Outer well width	a	$\pi/\sqrt{2}$	$[\hbar/\sqrt{mE_0}]$
Inner well width	b	0.03	$[\hbar/\sqrt{mE_0}]$
Barrier width	c	0.081	$[\hbar/\sqrt{mE_0}]$
Barrier height	V_b	800	$[E_0]$
Inner well depth (exact)	d_{exact}	36.95	$[E_0]$
Inner well depth (WKB)	d_{WKB}	1137	$[E_0]$
Detuning	ϵ	0.001–0.1	$[E_0]$
Tunnel coupling (exact, $\epsilon = 0$)	$t_0^{(exact)}$	0.0017	$[E_0]$
Tunnel coupling (WKB, $\epsilon = 0$)	$t_0^{(WKB)}$	0.0011	$[E_0]$

Table 6.2: Parameters of the modified square double-well potential. The width and height parameters refer to those shown in Figure 4.3. The characteristic energy E_0 is the ground state energy of a single square well of width a. The given parameters place the single-well energies at $0.002E_0$ above the bottom of the outer well for both the exact and WKB cases.

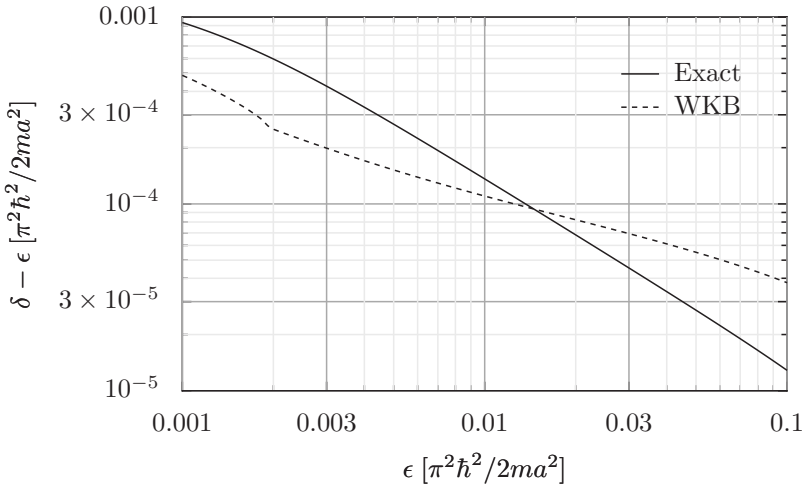

Figure 6.2: Numerical results for the modified square double-well potential. The WKB results (dotted line) imply an ϵ-dependent tunnel coupling for $\epsilon > 0.002E_0$. However, the exact results (solid line) represent an ϵ-independent tunnel coupling, suggesting that the WKB approximation is not valid for this potential.

i.e. the energy difference between the ground state and the bottom of the outer well, as predicted. However, the exact solution (solid line) shows no such transition and displays a dependence very close to the standard ϵ^{-1} across the entire range of detunings. These re-

sults imply that the observed transition is due to the breakdown of the WKB approximation, rather than an actual transition of the physical system.

In conclusion, our results show that the predictions of Section 4.3 are valid for typical potentials, but that the WKB approximation breaks down for exceptional potentials. These results suggest that the leading-order behavior of the tunnel coupling in a double-well is always independent of the detuning. However, an ϵ-dependence arising from higher order corrections is still possible, as discussed in the next chapter.

Chapter 7

Higher order corrections

In the previous chapter we saw that the WKB approximation only predicts a strongly detuning-dependent tunnel coupling in exceptional cases, and that the approximation breaks down in these cases, suggesting that the leading order behavior of the tunnel coupling is always ϵ-dependent. The numerical results of this chapter focus instead on detuning-dependent corrections to that leading order behavior. The simulations in Section 7.1 show the ϵ-dependence of the reduced Hamiltonian matrix elements. We then compare the actual ϵ-dependence of the energy shifts to those predicted by WKB for an infinite square double-well in Section 7.2.

7.1 Detuning-dependence of the reduced Hamiltonian

Numerical simulations were used to directly determine the matrix elements of the reduced Hamiltonian (Section 2.4) for a range of realistic detunings. The derivation of the reduced Hamiltonian requires a number of simplifications and approximations. Before looking for the small, ϵ-dependent corrections to tunnel coupling predicted by WKB, we must understand the types of corrections that are present in the reduced Hamiltonian.

The matrix elements were determined for two types of potentials, the piecewise parabolic potential described in Section 6.1, and a finite square double-well. First, an approximate full Hamiltonian was constructed by applying the finite difference method of Section 5.1 to the potential. The exact ground state wavefunctions for single-wells of the same shape (parabolic or finite square) were then determined. These wavefunctions, centered around the minima of the double well potential are the single-well states of Chapter 2, denoted by $|\phi_L\rangle$ and $|\phi_R\rangle$. To construct a localized basis, the following symmetric orthonormalization was used [18]:

$$|\psi_L\rangle = \frac{|\phi_L\rangle - g|\phi_R\rangle}{\sqrt{1-2gl+g^2}}, \tag{7.1}$$

$$|\psi_R\rangle = \frac{|\phi_R\rangle - g|\phi_L\rangle}{\sqrt{1-2gl+g^2}}, \tag{7.2}$$

$$l = \langle\phi_L|\phi_R\rangle, \tag{7.3}$$

$$g = \frac{1}{l}(1-\sqrt{1-l^2}). \tag{7.4}$$

The matrix elements $\langle\psi_L|H_h|\psi_L\rangle$, $\langle\psi_R|H_h|\psi_R\rangle$, and $\langle\psi_L|H_h|\psi_R\rangle$ were then determined directly, where H_h is the discretized Hamiltonian, for the full double-well potential.

7.1.1 Parabolic double-well results

For the parabolic double-well, the reduced Hamiltonian matrix elements described in Section 2.4 are shown in figures 7.1, 7.2, and 7.3. The σ_0 component shows a detuning-dependent shift of the energy levels of the reduced Hamiltonian, on the order of $10^{-4}t$. The σ_x component shows that t varies by about $10^{-3}t$ over the detuning range considered. Finally, the σ_z component varies from the assumed value of $\epsilon/2$ by a factor of about $10^{-2}t$. The primary detuning-dependence is thus in the deviation of σ_z from $\epsilon/2$. However, this deviation is linear in ϵ, implying that the s_z component can be written as $c\epsilon/2$ for some c. For $\epsilon \gg t$,

the correction to the tunnel splitting (2.64) becomes:

$$\delta - \epsilon \approx \frac{t^2}{2c\epsilon}. \tag{7.5}$$

As this correction simply multiplies the detuning by a constant, it does not change the detuning-dependence of the tunnel splitting. It is thus valid to use the tunnel splitting to determine small corrections to the tunnel coupling. However, it remains a possiblity that the corrections predicted within the reduced Hamiltonian model could be overshadowed by contributions from the neglected excited states.

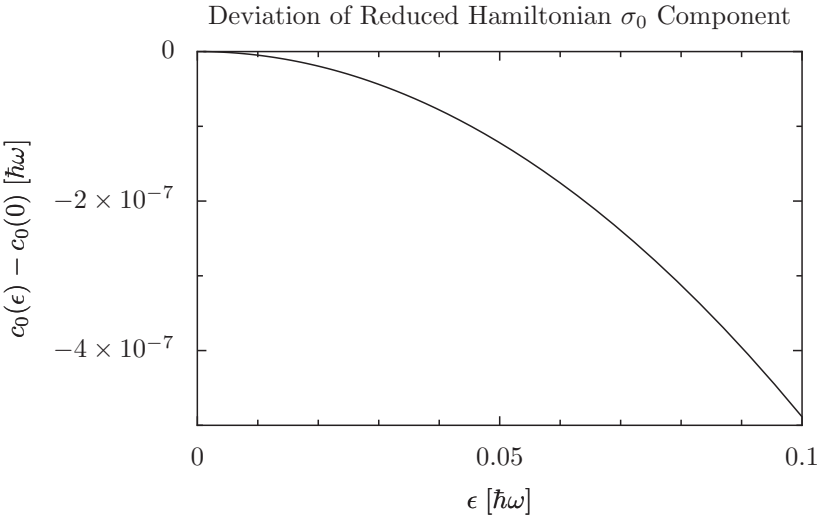

Figure 7.1: Deviation of the σ_0 component of the reduced Hamiltonian for the parabolic double-well. The deviation is taken relative to the $\epsilon = 0$ value of $0.4999534\hbar\omega$. This component represents a constant energy offset of the reduced Hamiltonian, relative to higher excited states, and has no effect on the tunnel splitting.

7.1.2 Finite square double-well results

The reduced Hamiltonian matrix elements for the finite square double-well are shown in figures 7.4, 7.5, and 7.6. The parameters for the potential are given in Table 7.1. As with the parabolic double-well, the finite square double-well shows small ϵ-dependent deviations from

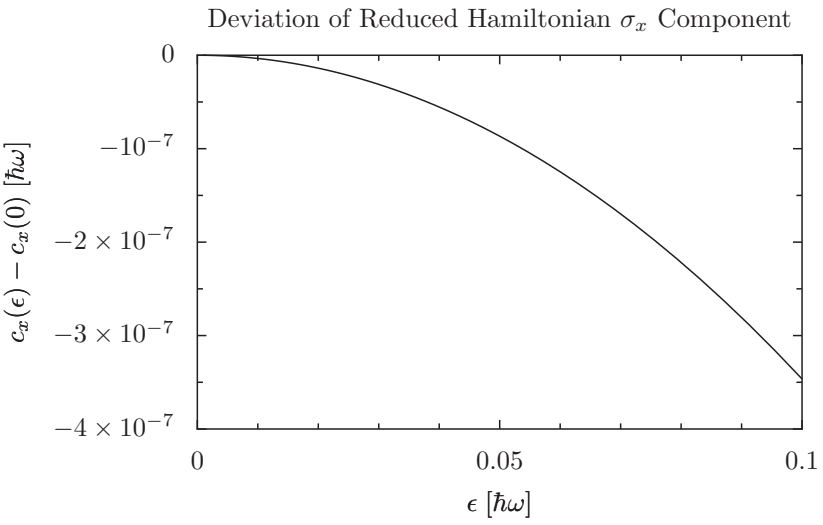

Figure 7.2: Deviation of the σ_x component of the reduced Hamiltonian for the parabolic double-well. This deviation is taken relative to the $\epsilon = 0$ value of $-8.179742 \times 10^{-4}\hbar\omega$. By definition, this component is $t/2$.

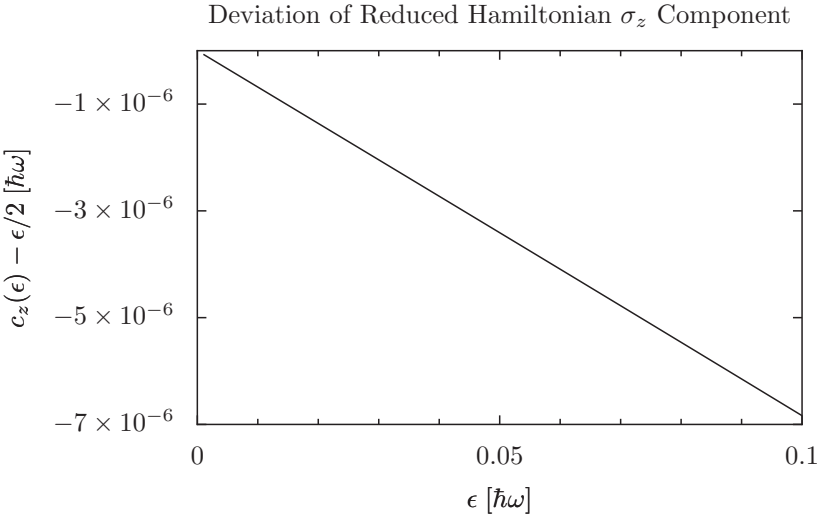

Figure 7.3: Deviation of the σ_z component for the reduced Hamiltonian for the parabolic double-well. This deviation is taken relative to the expected form of $\epsilon/2$. The deviation is small compared to t, but larger than the deviations of the other elements from their assumed values.

the assumed values of the matrix elements. The σ_0 component varies from its $\epsilon = 0$ value by $\sim 10^{-5}t$, the tunnel coupling varies by $\sim 10^{-8}t$, and the deviation of the σ_z component from

$\epsilon/2$ is linear and $\sim t$. Again, the σ_z component shows the most significant deviation from its assumed value. However, being linear in ϵ, the deviation does not change the ϵ-dependence of the tunnel splitting. Thus, as with the parabolic potential, the main contribution to the ϵ-dependence of the tunnel splitting is the tunnel coupling. However, this contribution is extremely small. These results provide a basis for comparison with the WKB prediction of the tunnel splitting, allowing us to determine if it is valid to write the tunnel splitting as a function of t, neglecting coupling to higher states. Also, the large deviation of the σ_z component from $\epsilon/2$ is noteworthy. If another potential showed a non-linear deviation of the σ_z component, but with a deviation of the same magnitude as that of the finite square double well, the relationship between tunnel coupling and tunnel splitting would be significantly modified.

Parameter		Value	Units
Single-well energy	E_0	1	$[E_0]$
Well width	a	$\pi\sqrt{2}/3$	$[\hbar/\sqrt{mE_0}]$
Barrier height	V_b	4	$[E_0]$
Barrier width	c	2.77	$[\hbar/\sqrt{mE_0}]$
Detuning	ϵ	0.001–0.1	$[E_0]$

Table 7.1: Parameters of the finite square double-well. The characteristic energy E_0 is the ground state energy of a finite square single-well of width a and height V_b.

7.2 Tunnel splitting corrections for a finite square well

We saw in Section 4.3.1 that for typical potentials, WKB predicts an ϵ-independent tunnel coupling with small ϵ-dependent corrections. These corrections arise from the Taylor expansion of the WKB phase shifts in the denominators of (4.54) and (4.55). For an infinite square double-well, the corrections predicted by WKB were compared to those determined by exact numerical methods. An infinite square double-well with the parameters given in Table 7.1 was used for this comparison.

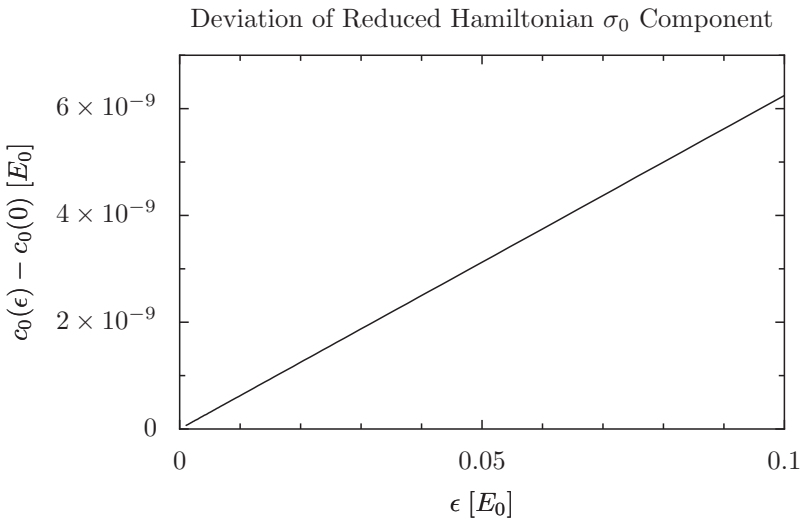

Figure 7.4: Deviation of the σ_0 component of the reduced Hamiltonian for the square double-well. This deviation is relative to the $\epsilon = 0$ value of 1.000157969. This component represents the shift in the reduced Hamiltonian energy levels relative to higher excited state and has no effect on the tunnel splitting.

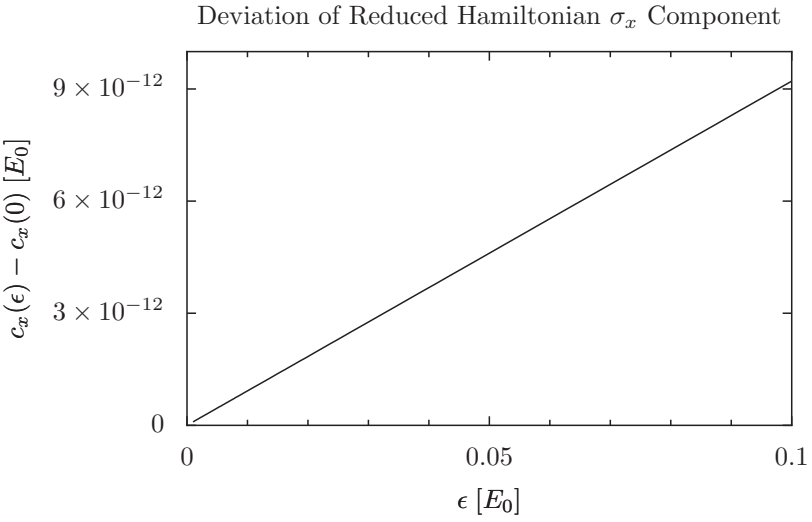

Figure 7.5: Deviation of the σ_x component (equal to $t/2$) of the reduced Hamiltonian for the square double-well. The deviation is taken relative to the $\epsilon = 0$ value of $-6.19266572 \times 10^{-4}$.

The WKB corrections are determined by substituting the Taylor expanded phase shifts into (4.54) and (4.55). For convenience, we consider the reciprocals of the phase shifts, $1/\delta_L$ and $1/\delta_R$. To second order, the phase integrals for a square double-well with wells of width

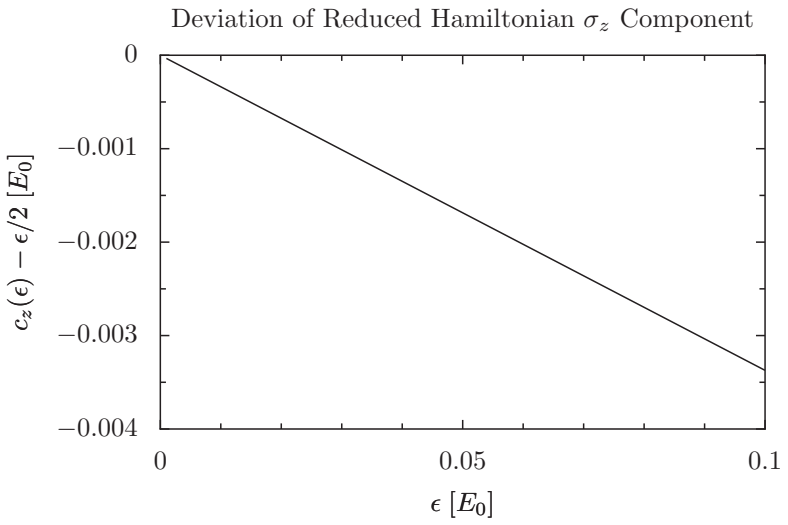

Figure 7.6: Deviation of the σ_z component of the reduced Hamiltonian for the square double-well. The deviation is taken relative to the assumed form of $\epsilon/2$. This deviation is very large, on the order of the tunnel coupling, but the linear ϵ-dependence does not change the relationship between tunnel splitting and tunnel coupling.

a are:

$$\begin{aligned}
\phi_{12}(E_R(\epsilon)) &= \frac{a\sqrt{2m}}{\hbar}\sqrt{E_R(\epsilon) - V_L} - \frac{\pi}{2} && (7.6)\\
&\approx -\frac{\pi\epsilon}{4\Delta} - \frac{\pi\epsilon^2}{16\Delta^2}, && (7.7)\\
\phi_{34}(E_L(\epsilon)) &= \frac{a\sqrt{2m}}{\hbar}\sqrt{E_L(\epsilon) - V_R} - \frac{\pi}{2} && (7.8)\\
&\approx \frac{\pi\epsilon}{4\Delta} - \frac{\pi\epsilon^2}{16\Delta^2}, && (7.9)\\
\Delta &= \frac{\pi^2\hbar^2}{8ma}, && (7.10)
\end{aligned}$$

where Δ is the offset between the WKB single-well ground state energy and the bottom of the well. Noting that

$$\phi'_{12}(E_L) = \phi'_{34}(E_R) = \frac{\pi}{4\Delta}, \tag{7.11}$$

The reciprocals of the WKB energy shifts are:

$$1/|\delta_L| = \frac{\pi^2}{4\Delta}\exp(2\theta_{23})\left(\frac{\epsilon}{\Delta}+\frac{\epsilon^2}{4\Delta^2}\right), \tag{7.12}$$

$$1/|\delta_R| = \frac{\pi^2}{4\Delta}\exp(2\theta_{23})\left(\frac{\epsilon}{\Delta}-\frac{\epsilon^2}{4\Delta^2}\right). \tag{7.13}$$

For a square double-well, WKB does not predict the correct magnitude for the single-well energies or tunnel coupling, so rather than checking the magnitude of the WKB phase shifts (7.12) and (7.13), it is necessary to check more qualitative features of their ϵ-dependence, such as curvature. No curvature ($\delta_{L/R} \propto \epsilon^{-1}$) corresponds to an ϵ-independent tunnel coupling, while any ϵ-dependence of the tunnel coupling will result in nonzero curvatures for $1/\delta_L$ and $1/\delta_R$.

The exact reciprocals of the energy shifts, determined using the finite difference method, are shown in Figure 7.7 and Figure 7.8, plotted against a straight line (dotted) for reference. Both $1/\delta_L$ and $1/\delta_R$ show a nonzero curvature. However, Equation (7.13) predicts that $1/\delta_R$ should curve down, when in fact it curves up. This discrepancy suggests that the accuracy of WKB approximation is not good enough to reliably determine the ϵ-dependence of the energy shifts.

The results of this chapter give significant insight into the relative effects of various contributions to the ϵ-dependence of the tunnel coupling and tunnel splitting. The results of Section 7.1 confirm that for both parabolic and square double-wells, within the model of a two-state reduced Hamiltonian, the primary influence on the ϵ-dependence of the tunnel splitting is the tunnel coupling, rather than ϵ-dependent deviations of other matrix elements. However, the results show that the σ_z component can vary significantly from its assumed value of $\epsilon/2$, suggesting that it might play a role in other potentials. The results of Section 7.2 show that the tunnel splitting of a square double-well deviates from what would be expected for an ϵ-independent tunnel coupling and negligible coupling to higher excited states. How-

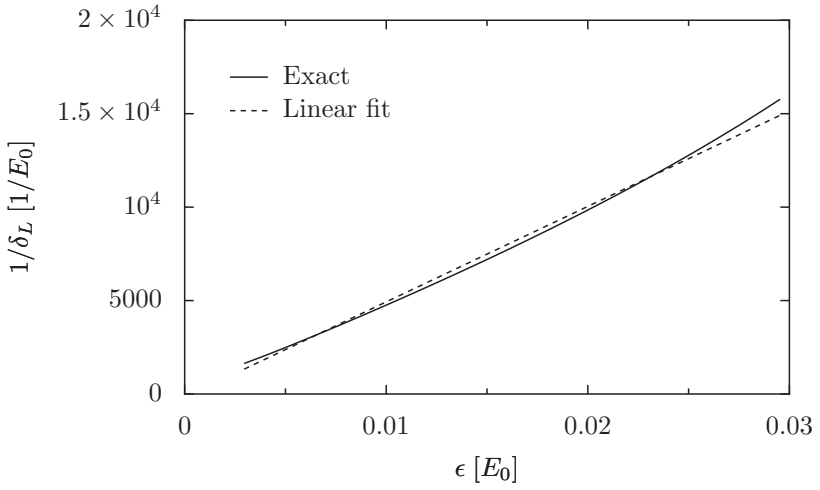

Figure 7.7: Reciprocal of the shift in the left well's energy due to tunneling for an infinite square double-well. The characteristic energy E_0 is the difference between the single-well ground state energy and the bottom of the well. The energy shift was determined numerically using the finite difference method. The best-fit straight line (dashed) is shown for comparison.

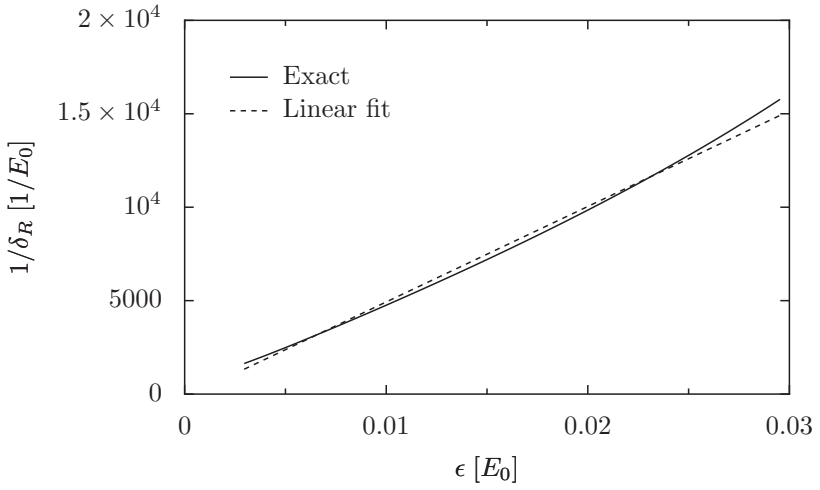

Figure 7.8: Reciprocal of the shift in the right well's energy due to tunneling for an infinite square double-well. The characteristic energy E_0 is the difference between the single-well ground energy and the bottom of the well. The energy shift was determined numerically using the finite difference method. The best-fit straight line (dashed) is shown for comparison.

ever, the observed results were qualitatively different from the WKB predictions, suggesting that the WKB approximation error is too large to accurately predict the ϵ-dependence of

corrections to the leading behavior of the tunnel splitting and tunnel coupling.

Chapter 8

Conclusion

We have discussed the behavior of an electron moving in a one-dimensional, double-well potential, with applications to quantum dot spin qubits. We began with a review of the effects of tunneling in a double-well, yielding a connection between detuning, tunnel splitting, and tunnel coupling. We then reviewed the quantization condition implied by the WKB approximation, and used it to derive expressions for the tunnel splitting in different types of potentials. We found that for typical potentials, WKB predicts energy shifts proportional to ϵ^{-1} plus higher order corrections, corresponding to a constant tunnel coupling with weak ϵ-dependent corrections. For an exceptional type of potential however, we found that WKB can predict energy shifts with a variety of leading order ϵ-dependencies, implying a strongly ϵ-dependent tunnel coupling. We then tested these predictions numerically for specific potentials.

Numerical simulations confirmed a weakly detuning-dependent tunnel coupling, but did not confirm the WKB predictions. The exceptional potentials for which WKB predicted strongly ϵ-dependent tunnel coupling did not show this behavior under full numerical solutions. This discrepancy is most likely due to large regions of the potentials containing very small WKB phase, thus invalidating the assumptions of the WKB approximation. Similarly,

some potentials showed small ϵ-dependent corrections, but the form of these corrections did not match the WKB predictions. The observed corrections were very small and likely overshadowed by the WKB approximation error for the regime considered.

Although WKB analysis did not yield the desired understanding of the detuning-dependence of the tunnel coupling, a number of interesting behaviors were observed that could be the subject of future study. Small ϵ-dependent corrections to the tunnel coupling were observed. The question of how these corrections depend on the shape of the wells and/or the barrier remains open. It could be the case that for some potentials, the corrections are large enough to become relevant. The derived WKB tunnel splitting expressions suggest that in a double-well with differently shaped wells, each well contributes a different energy shift to the tunnel splitting, implying an ϵ-dependent shift of both energy levels relative to higher excited states. This effect, if confirmed, could have interesting applications. Finally, the reduced Hamiltonian s_z component showed a significant deviation from its assumed value of $\epsilon/2$ for the square double-well. Such a deviation could modify the ϵ-dependence of the tunnel splitting, and has the potential to change the relationship between tunnel coupling and the exchange interaction. A further understanding of this effect would therefore be beneficial. Although consideration of the above corrections is unnecessary for a rough understanding of double quantum dots, as finer control of these devices becomes important, a more precise understanding incorporating these and similar corrections will become necessary.

Bibliography

[1] William F. Ames. *Numerical Methods for Parital Differential Equations*. Academic Press, Inc, 1977.

[2] R.C. Ashoori. Electrons in artificial atoms. *Nature*, 379:413–419, 1996.

[3] Carl M. Bender and Steven A. Orszag. *Advanced Mathematical Methods for Scientists and Engineers*. McGraw-Hill, Inc, 1978.

[4] Marc Bockrath, David H. Cobden, Paul L. McEuen, Nasreen G. Chopra, A. Zettl, Andreas Thess, and R.E. Smalley. Single-electron transport in ropes of carbon nanotubes. *Science*, 275(5308):1922–1925, 1997.

[5] Guido Burkard, Daniel Loss, and David P. DiVincenzo. Coupled quantum dots as quantum gates. *Physical Review B*, 59(3), January 1999.

[6] M. Ciorga, A.S. Sachrajda, P. Hawrylak, C. Gould, P. Zawadzki, S. Jullian, Y. Feng, and Z. Wasilewski. Addition spectrum of a lateral dot from coulomb and spin-blockade spectroscopy. *Physical Review B*, 61(16315), 2000.

[7] W.A. Coish and Daniel Loss. Quantum computing with spins in solids. *arXiv:cond-mat/0606550*, June 2006.

[8] Jane K. Cullum and Ralph A. Willoughby. *Lanczos Algorithms for Large Symmetric Eigenvalue Computations*. Birkhauser Boston, Inc, 1985.

[9] J.M. Elzerman, R. Hanson, J.S. Greidanus, L.H. Willems van Breveren, S. de Franceschi, L.M. Vandersypen, S. Tarucha, and L.P. Kouwenhoven. Few-electron quantum dot circuit with integrated charge read out. *Physical Review B*, 67(161308), 2003.

[10] M. Fricke, A. Lorke, J.P. Kotthaus, G. Medeiros-Ribeiro, and P.M. Petroff. Shell structure and electron-electron interaction in self-assembled inas quantum dots. *Europhys. Lett.*, 36(3), October 1996.

[11] L. Gaudreau, S.A. Studenikin, A.S. Sachrajda, P. Zawadzki, A. Kam, J. Lapointe, M. Korkusinski, and P. Hawrylak. Stability diagram of a few-electron triple dot. *Physical Review Letters*, 97(036807), 2006.

[12] Robert Gilmore. *Elementary Quantum Mechanics in One Dimension*. Johns Hopkins University Press, 2004.

[13] David J. Griffiths. *Introduction to Quantum Mechanics*. Pearson Education Inc., second edition, 2005.

[14] Paul Harrison. *Quantum Wells, Wires and Dots: Theoretical and Computational Physics of Semiconductor Nanostructures*. John Wiley and Sons, Ltd, 2nd edition, 2005.

[15] T. Hayashi, T. Fujisawa, H.D. Cheong, Y.H. Jeong, and Y. Hirayama. Coherent manipulation of electronic states in a double quantum dot. *Physical Review Letters*, 91(226804), 2003.

[16] E. A. Laird, J.R. Petta, A.C. Johnson, C.M. Marcus, A. Yacoby, M.P. Hanson, and A.C. Gossard. Effect of exchange interaction on spin dephasing in a double quantum dot. *Physical Review Letters*, 97(056801), July 2006.

[17] L. D. Landau and E. M. Lifshitz. *Quantum Mechanics (Non-relativistic Theory)*. Elsevier Science Ltd., third edition, 1977.

[18] D.C. Mattis. *The Theory of Magnetism*. Harper and Row, 1965.

[19] Michael A. Nielsen and Isaac L. Chuang. *Quantum Computation and Quantum Information*. Cambridge University Press, 2000.

[20] W. Nolting. *Quantenmechanik-Methoden und Anwendungen*. Grundkurs Theoretische Physik. Springer, 2004.

[21] J.R. Petta, A.C. Johnson, C.M. Marcus, M.P. Hanson, and A.C. Gossard. Manipulation of a single charge in a quantum double dot. *Physical Review Letters*, 93(186802), 2004.

[22] D. Schröer, A.D. Greentree, L. Gaudreau, K. Eberl, L.C.L. Hollenberg, J.P. Kotthaus, and S. Ludwig. An electrostatically defined serial triple quantum dot charged with few electrons. *Physical Review B*, 76(075306), 2007.

[23] Ioana Serban. *Nonlinearities in the quantum measurement process of superconducting qubits*. PhD thesis, LMU Munich, May 2008.

[24] Sander J. Tans, Michel H. Devoret, Hongjie Dai, Andreas Thess, Richard E. Smalley, L.J. Geerligs, and Cees Dekker. Individual single-well carbon nanotubes as quantum wires. *Nature*, 386:474–477, 1997.

[25] S. Tarucha, D.G. Austing, T. Honda, R.J. van der Hage, and LP Kouwenhoven. Shell filling and spin effects in a few electron quantum dot. *Physical Review Letters*, 77(3613), 1996.